



**AUSTRALIAN ATOMIC ENERGY COMMISSION  
RESEARCH ESTABLISHMENT  
LUCAS HEIGHTS**

**REVIEW OF GAMMA-RAY TRANSITIONS FROM  
keV NEUTRON CAPTURE**

**by**

**B.J. ALLEN**

**September 1970**

ISBN 0 642 99379 3



AUSTRALIAN ATOMIC ENERGY COMMISSION

RESEARCH ESTABLISHMENT

LUCAS HEIGHTS

REVIEW OF GAMMA-RAY TRANSITIONS FROM keV NEUTRON CAPTURE\*

by

B. J. ALLEN<sup>†</sup>

ABSTRACT

The study of gamma rays from neutron capture in the keV energy region provides information on the properties of individual resonances with keV spacing in light nuclei or nuclei near closed shells, and on the average behaviour of resonances in heavy nuclei. The effects of p and d-wave capture can be investigated across the periodic table, as can the neutron capture mechanisms. A variety of techniques are applicable in this energy range and these, with the results obtained, are reviewed in this paper.

\* Text of invited paper to A.P.S. meeting, Chicago, January 1970.

† Present address Physics Division, Oak Ridge National Laboratory.

National Library of Australia card number and ISBN 0 642 99379 3

CONTENTS

	<u>Page</u>
1. THERMAL AND RESONANCE CAPTURE GAMMA RAYS	1
2. EXPERIMENTAL TECHNIQUES	3
3. RESOLVED RESONANCE CAPTURE	4
3.1 2s-1d Shell	4
3.2 2p-1f Shell	4
3.3 E2 Transitions or d-Wave Capture	5
3.4 p and d-Wave Strength Functions	6
3.5 Distribution of Partial Radiative Widths	7
3.6 Resonance Asymmetry in Partial Capture Cross Section	8
4. AVERAGE NEUTRON CAPTURE	8
4.1 Averaging Experiments	8
4.2 Energy Dependence	9
4.3 Anomalous Bumps	10
5. CONCLUDING REMARKS	11
6. ACKNOWLEDGEMENTS	12
7. REFERENCES	12

Table 1	Survey of keV capture experiments
Table 2	Multipolarity of gamma ray transitions for capture in even-even targets
Table 3	Transitions to $5/2^-$ final states
Table 4	Transitions to $7/2^-$ final states

Figure 1	Nine decades of neutron capture
Figure 2	Resonance capture gamma ray spectra in $^{206}\text{Pb}$ . (Gamma ray spectra are obtained for each neutron resonance in this two parameter experiment)
Figure 3	Dual parameter system for the study of radiative keV neutron capture. (Gamma ray and time-of-flight pulses are analysed in coincidence and processed by an on-line computer)
Figure 4	The keV capture spectrum in $^{48}\text{Ti}$ . (The energies of the primary gamma rays from keV capture are shifted by the neutron resonance energies above the corresponding thermal (background) gamma ray energies)

continued...

CONTENTS (continued)

- Figure 5 Transitions to high spin ( $5/2^-$ ,  $7/2^-$ ) final states in  $^{41}\text{Ca}$ ,  $^{53}\text{Cr}$ ,  $^{57}\text{Fe}$ . (These transitions are not seen in the corresponding portions of the thermal capture spectra)
- Figure 6 Energy eigenvalues for single neutron states in nuclei with  $20 < A < 65$ . (Solid and open dots correspond to observed values for p and s final states which are populated most strongly in thermal and keV capture respectively. Solid lines are calculated single neutron energies)
- Figure 7 Schematic variation of neutron states across the periodic table. (At the zero binding of neutron shells, the appropriate strength function maximises, and E1 transitions link low lying shells)
- Figure 8 The keV capture spectra for targets of  $^{88}\text{Sr}$ ,  $^{90}\text{Zr}$ ,  $^{92}\text{Zr}$ ,  $^{94}\text{Zr}$ . (Strong transitions are observed to  $5/2^-$  ground states which are not observed in thermal capture)
- Figure 9 The p and d-wave strength functions. (Optical model calculations deviate substantially from the scattered experimental data)
- Figure 10 An  $\ell$ -wave analysis of keV capture cross sections in Zn. (To fit the energy dependence,  $S_2$  is required to be  $\sim$  zero. The derived value of  $S_2 \sim 2 \times 10^{-4}$  eV results in the d-wave cross section exceeding the capture cross section above 70 keV)
- Figure 11  $\chi$  squared distributions with 1,5, and 25 degrees of freedom
- Figure 12 Distribution of reduced partial radiative widths in  $^{56}\text{Fe}(n,\gamma)$ . (Transitions to the ground and first excited state doublet exhibit strong correlations over a 75 keV energy range)
- Figure 13 Partial capture cross section for  $^{208}\text{Pb}(\gamma_0,n)$ . (The asymmetry of the 41 keV resonance is interpreted in terms of a semi-direct interaction)
- Figure 14 The 50 keV averaged capture spectrum in Cu. (The uncertainty in the mean intensities is  $\sim 20\%$ , and comparable to the experimental error. The high energy enhancement observed in thermal capture is not present in the keV region)
- Figure 15 Comparison of reduced widths in  $^{59}\text{Ni}$ . (The correlation between (d,p) neutron widths and thermal capture radiative widths does not extend into the keV region)
- Figure 16 Variation of gamma ray intensities with neutron energies in Co. (Intermediate structure with width 10-20 keV is observed, though the resonance spacing is only 1.4 keV)
- Figure 17 Average NaI spectra for keV capture in Ta and Au. (The calculated shape for a statistical model interaction is shown, and contrasts with the anomalous bump at 5.5 MeV)
- Figure 18 Average capture spectra in Au. (The spectral shape is constant for neutron energies to 3.2 MeV)

## 1. THERMAL AND RESONANCE CAPTURE GAMMA RAYS

Neutron capture research extends over nine decades of energy - from cold and thermal meV fluxes to the  $d(t,n)$  reaction near 15 MeV. However most work has been at thermal energies, using high flux reactors and large thermal capture cross sections which permit gamma ray spectra to be obtained with minute quantities of separated isotopes. There are in fact some 50 groups throughout the world who pursue thermal capture gamma rays, mostly with Ge(Li) detectors.

In these nine decades of energy (Figure 1) the capture cross section varies from well-separated s-wave resonances, on which the statistical model is based<sup>(1)</sup>, through unresolved resonance regions where p,d and higher  $\ell$ -waves are important, to the giant resonance region and beyond where direct and semi-direct capture mechanisms<sup>(2)</sup> are called on to explain the magnitude of the cross sections. But even in the eV and keV regions evidence is accumulating which requires the presence of direct (or hard sphere) non-resonant effects<sup>(3,4)</sup>, resonant channel (valence neutron or external) capture<sup>(3,4)</sup>, and doorway (2p-1h) states from semi-direct interactions<sup>(5)</sup> which precede and sometimes compete with the complex nuclear states described by the statistical model in which all nucleons are involved in the excitation of the compound nucleus.

The thermal capture studies are important in that they have yielded a vast amount of nuclear data on energy levels and cascade schemes, spins and parities of low-lying states and so on<sup>(6)</sup>, as well as the gamma ray spectra which gave the first indication of a systematic variation in the capture mechanism across the periodic table<sup>(7)</sup>. However only a limited investigation of the neutron physics involved in thermal capture was possible, for the following reasons:

- (a) Thermal capture can be either a non-resonant reaction or one in which an indeterminate mixture of the tails of bound and unbound excited states contributes.
- (b) The observation of transitions to low lying excited states in the compound nucleus is limited by multipole selection rules operating on the two possible s-wave spin states, the wide variation of partial radiative widths, and the possibility of interference terms between the various radiative amplitudes<sup>(8)</sup>.
- (c) The correlation of capture radiative widths and the reduced neutron widths of final states (from the (d,p) reaction) is therefore not rigorous and it is also not possible to separate direct capture effects from channel capture.

The justification for the somewhat arduous task that faces the physicist when he turns to study resonance capture is the elimination of these limitations.

Additional bonuses are the isotopic identification of resonances by gamma ray spectra, the observation of a greater range of transitions through higher  $l$ -wave capture, and the determination of spin assignments of capture resonances. This last feat can be accomplished by measuring:

- (a) angular distributions of primary gamma rays to final states with known spin and parity  $(J_f^\pi)^{(9)}$ ,
- (b) population of low lying states by the gamma ray cascade<sup>(10)</sup>, and
- (c) resonance-resonance interference analysis<sup>(11)</sup>.

It is also possible to investigate channel capture by correlations of the partial radiative widths and the product of the reduced neutron widths of both capture and final states  $(\propto \Gamma_{nc}^0 \Gamma_{nf}^0)^{(12)}$ . The observation of asymmetry in the partial capture cross section resonance can lead to estimates of the direct capture component<sup>(13)</sup>, provided that corrections are made for resonance-resonance interference.

To date most resonance capture studies have been in the eV region on medium and heavy A nuclei, where the resonance spacing is in the range 10 - 100 eV. However there are many nuclides with resonance spacing in the keV region, those with light A or near closed shells, which warrant study and which by virtue of their simpler shell structure might deviate more seriously from statistical behaviour. Together with the increased interest in this energy range for fast reactor systems and nucleosynthesis research, we then have the justification for the even more arduous task of measuring keV capture gamma rays.

Resonance gamma ray spectra are analysed with the aim of obtaining information on their departure from the expected statistical behaviour. The statistical properties of interest are that:

- (a) The primary gamma ray decay spectrum should be smooth. That is, the broad features of the capture spectrum should be proportional to  $E_\gamma^3 \rho(E_c - E_\gamma)$ , where  $\rho(E_c - E_\gamma)$  is the density of final states<sup>(14)</sup>. Individual gamma ray intensities however should be proportional to  $\propto E_\gamma^3$ , assuming only E1 transitions contribute significantly.
- (b) The partial radiative widths should vary widely according to a chi-squared distribution with one degree of freedom<sup>(15)</sup>.
- (c) Correlations are not expected between the partial radiative widths and the reduced neutron widths of resonances and final states.

The results of keV capture experiments will be discussed in the following sections in terms of deviations from these properties.



## 2. EXPERIMENTAL TECHNIQUES

In referring to the keV region, a neutron energy range from a few keV to a few hundred keV is implied and these somewhat arbitrary limits will define the discussion in this paper. The lower bound of the keV region is reached by beams from fast choppers and linear accelerators. Resonance spectra have been measured to 5 keV, and recent Brookhaven results<sup>(16)</sup> have extended to 23 keV for  $^{92}\text{Mo} (n,\gamma)$ .

The Sc reactor filter used at Idaho Falls<sup>(17)</sup> provides a monoenergetic neutron beam at 1.95 keV with a FWHM of 700 keV. Fe and Si filters show promise of beams at 25 and 144 keV. However the Van de Graaff accelerator is the major source of fast neutrons with energies from 5 keV to the MeV region. Intense kinematically collimated monoenergetic fluxes are produced at 30 and 65 keV when Li and tritium targets are bombarded by protons at the threshold energy. Normally the accelerator is pulsed (2-50 ns at  $\sim 1$  MHz) and the time-of-flight method is used to measure neutron energies. The  $\text{Li}(p,n)$  reaction produces neutrons in the range 5-100 keV when bombarded at 10-20 keV above threshold<sup>(18)</sup>. Higher energies but lower yields and increased backgrounds can be obtained if required. However under these conditions the time-of-flight technique serves mainly to separate background and fast capture events.

The first measurements of keV capture spectra were made with a pulsed Van de Graaff accelerator by Bergqvist and Starfelt at Studsvik<sup>(19)</sup> and Firk and Gibbons at Oak Ridge<sup>(20)</sup>. Sodium iodide detectors were used to obtain the gross features of the capture spectra. The Swedish effort was directed to investigating the spectrum shape for heavy nuclei while gamma ray intensities were obtained at Oak Ridge for a number of nuclei with simple decay schemes (Figure 2). With the introduction of the Ge(Li) detector, work began at Lucas Heights on developing techniques to permit the high resolution study of resonance capture gamma ray spectra in the keV region<sup>(21)</sup>. The experimental arrangement is shown in Figure 3. The Ge(Li) detector is placed at  $0^\circ$  to the beam and shielded by a  $\text{B}_4\text{C}$ -loaded paraffin cone set through the centre of a massive annular capture target (50 cm from the neutron source). The simultaneous measurement of the neutron time-of-flight and gamma ray pulse heights allow capture spectra to be determined for either individual well spaced resonances or as an average over a number of resonances. In either case the gamma ray energy for a primary transition to a particular final state increases with neutron energy. This shift in gamma ray energy for resonances in the keV region can be observed readily with the Ge(Li) detector and has been used to identify resonances not resolved in the time-of-flight spectrum<sup>(22)</sup> (Figure 4).

The methods used at Lucas Heights have been necessitated by the relatively low capture cross sections at keV energies, the low efficiency of the Ge(Li) detector, and the sensitivity of the experiment to thermal and low energy neutrons. Because of the low efficiency of the Ge(Li) detector, large NaI detectors ( $\sim 12$  in  $\times$  8 in dia.) are still used to advantage where the gamma ray spectra are relatively simple, or when only small samples of separated isotopes are available for capture targets. Consequently Bergqvist et al. at Stockholm<sup>(23)</sup>, and Bird and co-workers at Lucas Heights continue to make further measurements with these detectors.

A survey of keV capture experiments is given in Table 1. Detector and neutron sources are noted, and the type of experiment is indicated.

### 3. RESOLVED RESONANCE CAPTURE

#### 3.1 2s-1d Shell

The wide resonance spacing and relatively simple decay spectra of nuclei in the 2s-1d shell permit the application of the high efficiency NaI detector to the measurement of capture gamma ray spectra. F, Na, Mg, Al, and S were studied by the Oak Ridge group<sup>(24,25,26)</sup>, and Bergqvist et al. in Sweden has made further measurements<sup>(23)</sup>. Both positive and negative parity states induced by s-wave and p-wave resonances were studied and branching ratios were obtained for several cases. The E1 and M1 transition strengths measured are in good agreement with results of charged particle reactions with other nuclides in this mass region, and the strengths of M1 and E1 transitions are comparable. However the ratio of reduced M1/E1 strengths is small ( $\sim 10^{-2}$ ) for even Z nuclei and much larger ( $\sim 10^{-1}$ ) for odd Z nuclei. Several resonance spectra are considerably at variance with statistical expectations. In particular the decay of the 27 and 50 keV resonances in F to a 2 MeV excited state, shows a consistent strength which implies a strong overlap between the capture and final states<sup>(24)</sup>. This is evidence for simple capture state configurations.

#### 3.2 2p-1f Shell

The Ge(Li) detector has been used in extensive measurements on nuclei in the 2p-1f shell. Resonance spectra to 5 keV have been measured at Argonne<sup>(27)</sup>, Brookhaven<sup>(28)</sup>, Livermore<sup>(29)</sup>, and Harwell<sup>(30)</sup> for Mn, Fe, Co and Cu using as neutron sources fast choppers and linear accelerators. In the 5-100 keV range the Lucas Heights group<sup>(31)</sup> have measured spectra from resolved resonances in Ca, Ti, Cr, and Fe. New transitions have been observed in many cases and information has been gained on the neutron capture mechanism and the effects of p- and d-wave neutrons.

It was for this mass region that Groshev et al.<sup>(7)</sup> had originally observed

anomalous thermal capture gamma ray spectra, and had later shown the correlation<sup>(32)</sup> between the intense high energy transitions and final states with large reduced neutron widths (from the (d,p) reaction). Lane and Lynn<sup>(3)</sup> found theoretically that the direct capture cross section should maximise at  $A \sim 52$ , and several attempts have been made to measure the direct component by the observation of interference effects with the partial gamma ray capture cross sections<sup>(32)</sup>. These experiments are really outside the 'keV energy region' as defined for this paper but some values obtained<sup>(29)</sup> for  $\sigma(\text{direct})$  at 1 eV are: 0 mb for  $^{55}\text{Mn}$ , 9 mb for  $^{59}\text{Co}$ , and 2.7 mb for  $^{63}\text{Cu}$ . The major problem is to minimise the resonance-resonance interference and in particular, interference from the unknown bound resonances. Auchampaugh<sup>(29)</sup> notes that not only is a wide resonance spacing required but also measurements should be made in the keV region to eliminate interference from bound levels.

### 3.3 E2 Transitions or d-Wave Capture

An important feature of the 5-100 keV experiments has been the observation of transitions to high spin final states ( $5/2^-$ ,  $7/2^-$ ) for even-even targets<sup>(33)</sup> (Figures 4,5). These transitions are not observed in s-wave thermal capture since M2 and E3 radiation would be involved. However these final states can be reached by E1 transitions after d-wave and M1 or E2 transitions after p-wave capture at keV energies (Table 2). The reduced widths are consistent with either the E1 or M1 possibility (Table 3), but require a  $\times 200$  enhancement factor over the Weisskopf single particle estimate for E2 radiation. Such enhancement had been unknown across the periodic table prior to the determination of the spin and parity of the p-wave 1.15 keV resonance in  $^{56}\text{Fe}$ . Chrien et al.<sup>(9)</sup> measured the strength of the E2 transition from the  $1/2^-$  resonance to the  $5/2^-$  final state and found it to be of the same order of enhancement (Table 4). This result for one transition may be a chance fluctuation, but there is also a problem of reconciling the capture cross section measurements in this mass region. Hockenbury et al.<sup>(35)</sup> concluded that the narrow capture resonances observed at keV energies must be p-wave, otherwise the d-wave strength function would be anomalously high. To date however there is no shell model explanation for such a major enhancement of E2 transitions, whereas d-wave capture is expected to maximise in this mass region because of the importance of single neutron states at zero binding energy.

The trend of capture gamma ray spectra for even-even targets depends markedly on the energies of  $p_{1/2}$ ,  $p_{3/2}$ , and  $s_{1/2}$  single particle shells in the 2s-1d shell and beyond<sup>(36)</sup>. The energies of the final states to which the strongest E1 transitions are observed in thermal capture are shown in Figure 6, and compared with the calculated energies of single neutron states. At the zero binding of the  $2p_{3/2}$  shell, keV capture data show strong E1 transitions

from p-wave resonances to  $s_{1/2}$  low lying states. A similar effect is expected in the 2p-1f shell ( $A \sim 60$ ) where the binding energy of the 2d shell goes to zero and E1 transitions from d-wave resonances can reach 2p and 1f final states, and in the 3s-2d shell ( $A \sim 90$ ) where the 3p neutron shell has zero binding, and E1 transitions can reach  $s_{1/2}$  and  $d_{3/2}$ ,  $d_{5/2}$  low lying states (Figure 7).

Strong transitions are indeed observed to  $5/2^-$  final states in  $^{88}\text{Sr}$ ,  $^{90}\text{Zr}$ ,  $^{92}\text{Zr}$  and  $^{94}\text{Zr}$  in keV measurements with NaI detectors<sup>(37)</sup> (Figure 8), but again there is the remote possibility that these may be enhanced E2 transitions from s-wave capture.

This simple shell model approach is reflected in the results obtained from optical model calculations which indicate maxima in the  $l$ -wave strength functions at the zero binding of the appropriate s, p and d neutron shells. The behaviour of the s-wave strength function is well known, and experimental results are in good agreement with calculations. However this is not the case for  $l > 0$ .

### 3.4 p and d-Wave Strength Functions

Optical model calculations of p<sup>(38)</sup> and d-wave<sup>(39)</sup> neutron strength functions deviate substantially from the somewhat sparse empirical data. In the  $A \sim 60$  region, the calculated strength functions (in units of  $10^{-4} \text{ eV}^{-\frac{1}{2}}$ ) are  $S_1 \sim 1.2$  and  $S_2 \sim 7$ . However only experimental results for  $S_1$  are available and these are considerably lower<sup>(35)</sup>, that is  $S_1 \sim 0.1$  (Figure 9).

Rough estimates of the p and d-wave strength function can be derived from an analysis of keV capture gamma ray spectra if the spins and parities of low lying final states are known. In particular transitions are observed to both positive and negative parity low lying states in  $^{65}\text{Zn}$ <sup>(31)</sup>, and average transition strengths can be calculated if a value of the E1/M1 ratio is assumed. For  $E1/M1 \sim 10$ , estimates are  $S_1 \sim 0.04$  and  $S_2 > 2$ . These values are based mainly on the strengths of transitions to the ground and first excited states (absent in thermal capture) and the weakness of transitions to positive parity states.

This result is in fair agreement with expectations, but calls for a substantial reduction in  $S_2$  for  $E_n > 60$  keV; otherwise the capture cross section is exceeded. While traditionally the E1/M1 ratio  $\sim 10$ <sup>(14)</sup>, recent results across the periodic table, and in particular for the 1.15 keV resonance in  $^{56}\text{Fe}$  ( $E1/M1 \sim 1$ )<sup>(9)</sup>, indicate that this assumption may not always be valid. Using the ratio of unity gives  $S_1 \sim 0.7$  and  $S_2 \sim 0$ . This is a rather high value of  $S_1$  for this mass region, and a completely anomalous result for  $S_2$  in terms of theory. The result however is in agreement with the  $l$ -wave analysis of the energy dependence of the natural zinc capture cross section (Figure 10), but is in general contradiction to similar analyses for neighbouring nuclei<sup>(40)</sup>.

### 3.5 Distribution of Partial Radiative Widths

It has long been established for heavy nuclei that the reduced neutron widths of resonances show wide variations and that the distribution of widths can be described by a  $\chi$ -squared distribution (see Figure 11) with one degree of freedom ( $\nu=1$ )<sup>(15)</sup>. That is,

$$P(\chi, \nu/2) d\chi = \Gamma(\nu/2)^{-1} (\chi \nu/2)^{\nu-1} \exp(-\chi \nu/2) \nu/2 d\chi ,$$

where

$$\chi = \Gamma_n^0 / \langle \Gamma_n^0 \rangle$$

and  $\Gamma(\nu/2)$  is the gamma function. One of the major contributions of resonance capture gamma ray experiments in the eV region has been to show that in general the partial radiative widths obey this same distribution<sup>(41)</sup>. Both neutron and gamma ray decay modes then appear to be single channel processes.

To date, however, there have been no analyses for nuclei with keV resonance spacing. Garg et al.<sup>(42)</sup> have made extensive total cross section measurements for many such nuclei and find that the s-wave resonance spacing is in good agreement with the predictions of the real symmetric Hamiltonian matrix model, with randomly distributed matrix elements. On this basis, a  $\nu=1$  distribution for partial radiative widths might well be expected.

The experimental difficulties are formidable in the keV region, and complicated by the presence of p and d-wave capture. But results are becoming available for a number of nuclei in the  $40 < A < 70$  mass region, which may indicate the distribution of the partial radiative widths for these nuclei. Partial widths have been obtained for many transitions over nominally six resonances in  $^{56}\text{Fe}$ <sup>(31)</sup>. The term 'nominally' is used because it is probable that unresolved s, p and/or d-wave resonances also contribute to the observed resonance spectra in a number of cases.

Making the assumption that s-wave capture is responsible for most of the observed strength, and that M1 widths (from the 1.15 keV p-wave resonance and any others) are enhanced and comparable in strength to E1 widths, the variation of transitions to nine  $1/2^-$ ,  $3/2^-$  final states from 'six' resonances can be obtained. Reducing the widths by the  $E_\gamma^3$  factor produces a population of 54 reduced widths, which are distributed as shown in Figure 12. The overall distribution appears to be the sum of two dissimilar distributions, and if those widths associated with  $\gamma_0$  and  $\gamma_1$  (ground and first excited state transitions) are removed a distribution with between 1 and 2 degrees of freedom remains. The  $\gamma_0$  and  $\gamma_1$  widths are seen to fit a distribution with approximately 16 degrees of freedom (see inset, Figure 12).

These results are based on a number of simplifying assumptions, but nevertheless indicate the presence of a high degree of correlation between transitions to the ground and first excited states, over a neutron energy range of about 75 keV.

### 3.6 Resonance Asymmetry in Partial Capture Cross Section

A reaction which seems well suited for measurements of the direct capture cross section is  $^{207}\text{Pb}(n,\gamma)^{208}\text{Pb}$ . In particular the 41 keV,  $1^-$  resonance is well separated from the other s-wave resonances and from the influence of any bound states. Measurement of the asymmetry of this resonance provides a measure of the direct capture cross section. The  $^{207}\text{Pb}(n,\gamma)$  reaction was studied at Oak Ridge with a large NaI crystal and results were analysed at Lucas Height<sup>(43)</sup>; a value of 0.2 mb was found for the direct cross section (0.04 b at 1 eV). Studies at Livermore<sup>(44)</sup> of the inverse  $^{208}\text{Pb}(\gamma_0,n)$  reaction were improved by a factor of 10 in energy resolution and confirmed the existence of the asymmetry (Figure 13). However these results were some two orders of magnitude greater than that predicted by the Lane and Lynn formalism. The asymmetry was therefore analysed by including interference between the direct and semi-direct (or doorway) interactions as formalised by Longo and Saporetti<sup>(2)</sup>. The capture cross section is given by:

$$\sigma(n,\gamma_0) = \pi/k_n^2 \cdot g_n \left| D - \frac{(\bar{\Gamma}_\gamma \bar{\Gamma}_n)^{\frac{1}{2}}}{(E_n + B - \bar{E}) + \frac{1}{2}i\bar{\Gamma}} - \frac{e^{-i\Phi}(\Gamma_n \Gamma_{\gamma_0})^{\frac{1}{2}}}{(E_n - E_0) + \frac{1}{2}i\Gamma} \right|^2,$$

where  $k_n$  and  $g_n$  are the neutron wave number and statistical factor,

$B$  is the neutron separation energy in  $^{208}\text{Pb}$ ,

$\bar{\Gamma}$ ,  $\bar{\Gamma}_n$ ,  $\bar{\Gamma}_\gamma$  are the widths of the giantdipole resonance at energy  $\bar{E}$

and  $\Gamma$ ,  $\Gamma_n$ ,  $\Gamma_\gamma$  are the widths of the compound nucleus resonance at energy  $E_0$ .

The resulting non-resonant cross section, 3-4 mb, was found to be in much better agreement with the semi-direct prediction.

The measurement of the  $^{207}\text{Pb}(\gamma_0,n)$  cross section up to 1200 keV has also been accomplished by this excellent technique<sup>(45)</sup> and evidence has been found in favour of the existence of a broad doorway state (300 keV envelope of capture resonances) previously suggested in elastic scattering measurements.

## 4. AVERAGE NEUTRON CAPTURE

### 4.1 Averaging Experiments

The wide fluctuations of partial radiative widths from resonance to

resonance has already been discussed in the preceding section. In order then to observe systematic effects in the capture spectra with energy or mass number it is necessary to eliminate these fluctuations by measuring spectra from a large number of resonances to obtain average intensities. Alternatively average spectra can be measured directly from the excitation of many unresolved resonances.

The  $\chi$ -squared distribution with  $\nu=1$  best describes the variation of partial radiative widths. However the average value of a partial radiative width over  $\nu$  resonances falls on a  $\chi$ -squared distribution with  $\nu$  degrees of freedom. This distribution approaches a gaussian for  $\nu$  large, and the relative uncertainty of the average width is  $\sim (2/\nu)^{\frac{1}{2}}$  (see Figure 11).

Average capture experiments have been performed at several energy ranges. The internal  $^{10}\text{B}$  filter technique has been used extensively at Argonne<sup>(46)</sup> to obtain average capture spectra from an eV neutron flux with a FWHM of  $\sim 400$  eV. Such measurements generally involve only s-wave capture and have shown a systematic relationship between the strengths of E1 and M1 transitions. Similar work will be possible with the Sc filter method used at Idaho Falls<sup>(17)</sup>, which provides an external beam at 1.95 keV (FWHM = 700 eV). The limited neutron energy range restricts the application of these methods to heavy nuclei with close resonance spacing.

#### 4.2 Energy Dependence

Many average capture measurements have been carried out in the 5-100 keV range and beyond, yielding important results. Ge(Li) studies of Cu and Ni at Lucas Heights<sup>(21,47)</sup> showed that the high energy transition strengths observed in thermal capture are substantially reduced (Figure 14). In fact the average transition strengths revealed an energy dependence consistent with the  $E_{\gamma}^3$  expected from the statistical model. The correlation between thermal capture partial widths and the reduced neutron widths of  $\ell_n = 1$  final states therefore vanishes for average partial widths in the keV region (see Figure 15). This result suggests then that channel capture, which is a resonance effect, is not the cause of the non-statistical thermal spectra. The alternative mechanism for thermal capture is direct capture, which results in the interference discussed in Section 3.2.

The energy dependence found for Zn<sup>(31)</sup> was midway between  $E_{\gamma}^3$  and the  $E_{\gamma}^5$  dependence observed for Pt and other heavy nuclei by Bollinger and Thomas<sup>(47)</sup>. This latter dependence is predicted on the basis of the giant resonance contribution to the capture cross section. However other results<sup>(31)</sup> for Sc, V, Mn and Co reveal a range of dependences, which implies the presence of configuration effects. The variation of the partial radiative widths in Co with neutron energy is characteristic of this. Intermediate structure with width about 10-20 keV

is apparent for a number of gamma rays (Figure 16), though the s-wave resonance spacing is 1.4 keV, and devoid of any grouping effect.

#### 4.3 Anomalous Bumps

Bergqvist and Starfelt made an extensive investigation of fast capture gamma ray spectra from unresolved resonances in the mass ranges  $110 < A < 130$ <sup>(48)</sup> and  $180 < A < 210$ <sup>(49)</sup>. A feature of these results was the appearance of an 'anomalous bump' in the gamma ray spectrum which appeared at Ag and Ta, and maximised in each case at Cs and Tl (Figure 17). This effect was found to be independent of neutron energy<sup>(50)</sup> up to  $\sim 4$  MeV (for Au) (Figure 18), ruling out the possibility of a direct interaction. The bump has also been observed in  $(d,p\gamma)$ <sup>(51,52)</sup> and  $(\gamma,\gamma)$ <sup>(53)</sup>, above and below the neutron threshold, and for  $(p,p^1\gamma)$ <sup>(55)</sup>.

Early attempts to explain the effect in terms of the statistical model with various level density and gamma ray energy dependences failed. However Starfelt<sup>(55)</sup> was able to account for the 'bump' if it was assumed that an M1 giant resonance with 1 per cent of the E1 giant resonance strength was present at 5.5 MeV. Such a resonance could result from M1 transitions (spin flip) between shells split by the spin-orbit interaction ( $g9/2 \rightarrow 7/2$ ,  $h11/2 \rightarrow 9/2$ ,  $i13/2 \rightarrow 11/2$ ). Bartholomew et al.<sup>(52)</sup> later suggested that the effect is due to the formation of doorway or  $1p-2h$  states which emit E1 radiation on p-h annihilation, the centre of gravity energy differences between single particle shells ( $s \leftrightarrow p$ ,  $d \leftrightarrow f$ ,  $g \leftrightarrow h$ ) being 5-6 MeV. Accumulated experimental evidence indicates that the bump mainly results from primary, E1 gamma rays in this energy range<sup>(56,57)</sup>, emitted as the nucleus enters one of several available doorway states with a precompound nucleus decay probability for an E1 (or M1) transition to a lower shell.

A similar explanation is given by Rimawi et al.<sup>(58)</sup> for the differences between the s and p-wave resonance spectra observed in  $^{93}\text{Nb}(n,\gamma)$ . Four possible p-h configurations exist for p-wave capture, but only one for s-wave. As the p-h annihilation energy is about 6-7 MeV, the  $l=1$  spectra exhibit high energy E1 enhancement while a statistical spectrum is observed for  $l=0$  resonances. Channel capture is ruled out as an alternative explanation because of the lack of correlation between the partial radiative widths and the reduced neutron resonance widths.

If the doorway interpretation is correct, then capture measurements in the keV region should show an increasing high energy spectral component corresponding to the increase in the p-wave capture cross section with neutron energy. This component should reduce when the neutron energy exceeds that of the doorway state, or alternatively when the d-wave capture cross section becomes substantially greater than the p-wave.



A similar argument was made by Groshev<sup>(61)</sup> for the  $^{62}\text{Ni} (n,\gamma)$  reaction. However in this instance keV measurements<sup>(47)</sup> showed that the doorway state did not exist, although a single low energy resonance may have the expected configuration.

The doorway states postulated for Nb and Au differ in that for the former case doorway states occur only through p-wave capture while in the latter case there is a sequence of doorway states formed which is effectively independent of the neutron energy and angular momentum involved.

## 5. CONCLUDING REMARKS

The analysis of keV capture experiments in the  $40 < A < 70$  region cannot proceed without clarification of the role of p and d-wave neutron interactions. More detailed measurements are required with angular distributions where possible to identify the multipolarity of primary transitions, and so attain reliable estimates of average E1, M1 and E2 transition strengths for this mass region. The p and d-wave contributions to capture at keV energies can then be estimated.

The inverse  $(\gamma_0, n)$  reaction is well suited to determine, by differential capture cross section measurements, the  $l$ -wave resonance spins. As s-wave resonances in even-even targets are expected to have negligible radiative widths for transitions to the  $7/2^-$  ground states, the  $(\gamma_0, n)$  reaction therefore proceeds through mainly d-wave resonances. In the  $^{48}\text{Ti} (n,\gamma)$  reaction, a suspected d-wave resonance lying within a few keV of the 37 keV s-wave resonance could be reached by the inverse reaction  $^{48}\text{Ti} (\gamma_0, n)$  and its spin determined from an angular distribution measurement. Such an experiment could result in the first positive identification of a d-wave resonance.

Improved resolution capture cross section measurements are also needed for keV nuclei to resolve some of the  $l$ -wave capture problems. The superposition of narrow p or d-wave resonances on broad s-wave resonances has been observed in a number of capture cross sections and evidence for such effects in gamma ray spectra is found for Ti and Fe, where transitions to high spin states are observed for neutron energies very close to known s-wave resonances. The 10 keV resonance observed in  $^{48}\text{Ti} (n,\gamma)$  by the energy shift of primary gamma rays<sup>(22)</sup> also requires verification in capture cross section measurements. The value of Ge(Li) detectors for observing low energy resonances is in question here.

Measurements on even Z nuclei in this same mass region should yield further estimates of the distribution of partial radiative widths for keV nuclei. However improved resolution of  $l$ -wave resonances is required. Correlation studies between the partial radiative widths and the reduced resonance neutron widths are needed to determine the extent of the channel capture mechanism in this mass region.

There have been no keV capture measurements in the  $N = 82$  region, where thermal studies have indicated a high correlation between  $\Gamma_{\gamma i}$  and the reduced neutron widths of the final states.

The keV measurements obtained to date rely on thermal capture results for absolute normalisation, assuming that all or some fraction of the thermal transition strength is present in the same energy range in resonance capture. Substantial errors are therefore introduced and a need arises for absolute measurements of partial widths using well determined 'calibration' resonances for normalisation (such as the 41 keV resonance in  $^{207}\text{Pb}(n,\gamma)$ , for which  $\Gamma_{\gamma} = 5.5$  eV).

Further measurements of resonance shapes are required, in order to gain more information on interference effects of direct, semi-direct and resonance capture cross sections. The 41 keV shape experiment for  $^{208}\text{Pb}$  needs to be confirmed for other resonances in Pb and further measurements should be made across the periodic table wherever large resonance spacings are available. As interference effects are averaged out when a number of gamma rays are included in the yield curve, the  $(\gamma_0, n)$  experiments are particularly suited for this work.

In the nuclear data field, there is a general need for gamma ray spectra from keV neutron capture, particularly for the light structural elements. These data are used for shielding calculations for fast reactor systems which at present rely on estimates based on the statistical model.

Neutron capture research separates into two broad experimental areas, the eV and the keV regions, where different neutron sources are used and different targets investigated. But each region complements the other, and each contributes to our understanding of the neutron capture reaction for a wide range of nuclei.

## 6. ACKNOWLEDGEMENTS

The author is grateful to Dr. J. R. Bird for a number of private communications on the subject matter of this paper.

## 7. REFERENCES

1. Goldstein, H. (1963). - Fast Neutron Physics, Interscience, Vol.II, 1525.
2. Brown, G. E. (1964). - Nucl. Phys. 57:339.
- Clement, C. F., Lane, A. M. and Rook, J. R. (1965). - Nucl. Phys. 66:273-293.
- Carlson, R. V. and Daly, P. J. (1967). - Nucl. Phys. A102:177.
- Longo, G. and Saporetto, F. (1968). - Il Nuovo Cimento, LVIB:264.
- Bergqvist, I., Lundberg, B., Nilsson, L. and Starfelt, N. (1966). - Phys. Letters 19:670.
- Sperber, D. (1969). - Phys. Rev. 184:1201.

3. Bird, J. R., Gibbons, J. H. and Good, W. M. (1962). - Int. Symp. on Direct Interactions and Nuclear Reaction Mechanisms. Padova, Italy.  
Lane, A. M. and Lynn, J. E. (1960). - Nucl. Phys. 17:563,586.
4. Lynn, J. E. (1968). - Theory of Neutron Resonance Reactions. Oxford.  
pp.326,333.
5. Feshbach, H., Kerman, A. K. and Lemmer, R. H. (1967). - Annals of Physics, 41:230-286.
6. See for example Bartholomew et al. (1967). - Nuclear Data, 3:367.
7. Groshev, L. V., Demidov, A. M., Lutsenko, V. N. and Pelekhov, V. I. (1959). - Atlas of  $\gamma$ -Ray Spectra from Radiative Capture of Thermal Neutrons, Pergamon Press.
8. Lone, M. A., Chrien, R. E., Wasson, O. A., Beer, M., Bhat, M. R. and Muether, H. R. (1968). - Phys. Rev. 174:1512.
9. Chrien, R. E., Bhat, M. R. and Wasson, O. A. (1969). - BNL 14104.
10. Ponitz, W. P. (1966). - Zeit. fur Physik, 197:262, see also Ref. 8.
11. Newson, H. W. and Gibbons, J. H. (1963). - Fast Neutron Physics, Inter-science, Vol. II, p.1601.
12. Lane, A. M. (1969). - Proc. Symp. on Neutron Capture  $\gamma$ -Ray Spectroscopy, Studsvik, August 1969. I.A.E.A. Vienna, p.513.
13. See Ref. 4, p.339.
14. Bartholomew, G. A. (1961). - Ann. Rev. Nucl. Sci. 11:259.
15. Porter, C. E. and Thomas, R. G. (1956). - Phys. Rev. 104:483.
16. Mughabghab, S. F., Chrien, R. E., Wasson, O. A., Garber, D. I. and Bhat, M. R. (1970). - BAPS II, 15(1).
17. Greenwood, R. C., Harlan, R. A., Helmer, R. G. and Reich, C. W. (1969). - Proc. Symp. on Neutron Capture  $\gamma$ -Ray Spectroscopy, Studsvik, August 1969, I.A.E.A. Vienna, p.607.
18. Gibbons, J. H. and Newson, N. W. (1960). - Fast Neutron Physics, Inter-science, Vol. I, p.133.
19. Bergqvist, I. and Starfelt, N. (1961). - Nucl. Phys. 22:513.
20. Firk, F. W. K. and Gibbons, J. H. (1966). - Proc. Saclay Symp. on Neutron Time of Flight Methods, p.213.
21. Allen, B. J. (1968). - Nucl. Phys. A111:1.
22. Bird, J. R., Kenny, M. J. and Allen, B. J. (1968). - Phys. Letters 27B:638.
23. Lundberg, B., Nystrom, G. and Bergqvist, I. (1969). - Proc. Symp. on Neutron Capture  $\gamma$ -Ray Spectroscopy, Studsvik, August 1969. I.A.E.A. Vienna, p.667.
24. Bird, J. R., Biggerstaff, J. A. and Good, W. M. (1965). - Phys. Rev. 138:B20.
25. Bird, J. R., Gibbons, J. H. and Good, W. M. (1962). - Phys. Letters, 1:262.

26. Bergqvist, I., Biggerstaff, J. A., Gibbons, J. H. and Good, W. M. (1967). -  
Phys. Rev. 158:1049; 1965 - Phys. Letters 18:323.
27. Prestwich, W. W. and Cote, R. E. (1967). - Phys. Rev. 155:1223.
28. Wasson, O. A., Garg, J. B., Chrien, R. E. and Bhat, M. R. (1968). - BNL 12268.  
Wasson, O. A., Bhat, M. R., Chrien, R. E., Lone, M. A. and Beer, M. (1966). -  
Phys. Rev. Letters, 17:1220.
29. Auchampaugh, G. F. (1968). - UCRL-50504.
30. Thomas, B. W., Uttley, C. A. and Rae, E. R. (1968). - AERE-PR/NP14, p.23.
31. Allen, B. J., Bird, J. R. and Kenny, M. J. (1969). - AAEC-E200.
32. Groshev, L. V., Demidov, R. M. and Shadiev, N. (1966). - Sov. Jour. Phys. 3:319.
33. See for example Refs. 27,28,29.
34. Bird, J. R., Allen, B. J. and Kenny, M. J. - AAEC-TM511; Proc. Int. Symp.  
on Neutron Capture  $\gamma$ -Ray Spectroscopy, Studsvik, August 1969,  
I.A.E.A. Vienna, p.587.
35. Hockenbury, R. W., Bartolome, Z. M., Moyer, W. R., Talarezak, J. R. and  
Block, R. C. (1969). - Phys. Rev. 178:1746.  
Morgenstern, J., Alves, R. N., Julien, J. and Samour, C. (1969). - Nucl.  
Phys. A123:561.
36. Bird, J. R. (1969). - Proc. Int. Conf. Properties of Nuclear States,  
Montreal, p.782.
37. Bird, J. R. (1970). - private communication.
38. Buck, B. and Perey, F. (1962). - Phys. Rev. Letters, 8:444.
39. Auerbach, E. H. and Perey, F. (1962). - BNL-765.
40. Musgrove, A. R. de L. (1969). - AAEC-E198.
41. See summary of results in R. E. Chrien - BNL 13884, Symp on Neutron  
Capture  $\gamma$ -Ray Spectroscopy, Studsvik, August 1969. p.627.
42. Garg, J. B., Rainwater, J. and Havens, W. W. Jr. (1969). - EANDC (US) - 54'L',  
CR-1860.
43. Broomhall, G. J. and Bird, J. R. (1968). - Nucl. Phys. A121:329.
44. Bowman, C. D., Baglan, R. J. and Berman, B. L. (1969). - Phys. Rev. Letters,  
23:796.
45. Bowman, C. D., Baglan, R. J. and Berman, B. L. (1969). - UCRL-71988.
46. Bollinger, L. M. and Thomas, G. E. (1968). - Phys. Rev. Letters, 21:233.  
Bollinger, L. M. (1968). - Proc. Int. Symp. on Nuclear Structure, Dubna, 1968.
47. Allen, B. J., Kenny, M. J. and Sparks, R. J. (1968). - Nucl. Phys. A122:220.
48. Bergqvist, I. and Starfelt, N. (1962). - Nucl. Phys. 39:529.
49. Bergqvist, I. and Starfelt, N. (1962). - Nucl. Phys. 39:353.
50. Lundberg, B. and Starfelt, N. (1965). - Nucl. Phys. 67:321.
51. Bartholomew, G. A., Earle, E. D., Ferguson, A. J. and Bergqvist, I. (1967). -  
Phys. Letters, 24B:47.

52. Bartholomew, G. A., Bergqvist, I., Earle, E. D. and Ferguson, R. J. (1970). - Can. J. Phys. 48(6):686.
53. Moreh, R. and Wolf, A. (1969). - Proc. Symp. on Neutron Capture  $\gamma$ -Ray Spectroscopy, Studsvik, August 1969. I.A.E.A. Vienna. p.483.
54. Bartholomew, G. A. (1969). - Proc. Symp. on Neutron Capture  $\gamma$ -Ray Spectroscopy, Studsvik, August 1969. I.A.E.A. Vienna. p.553.
55. Starfelt, N. (1964). - Nucl. Phys. 53:397.
57. Bartholomew, G. A., Earle, E. D. and Gunye, M. R. (1967). - Can. J. Phys. 45:1517,2063.
58. Rimarwi, K., Chrien, R. E., Garg, J. B., Bhat, M. R. Garber, D. I. and Wasson, O. A. (1969). - Phys. Rev. Letters, 23:1041.
59. Groshev, L. M. and Demidov, A. M. (1967). - Sov. Jour. Phys. 4:558.
60. Kennett, T. J., Bollinger, L. M. and Carpenter, R. T. (1958). - Phys. Rev. Letters, 1:76.
61. Bergqvist, I. and Starfelt, N. (1962). - Arkiv for Fysik, 23:40.
62. Bird, J. R. (1968). - Nucl. Phys. A120:113.
63. Bowman, C. D., Sidhu, G. S. and Berman, B. L. (1968). - URCL-14942,70473.
64. Bergqvist, I. (1962). - Arkiv for Fysik. 23:417.
65. Biggerstaff, J. A., Bird, J. R. Gibbons, J. H. and Good, W. M. (1967). - Phys. Rev. 154:1136.



TABLE 1  
SURVEY OF keV CAPTURE EXPERIMENTS

Target	Neutron Energy <sub>0</sub> (keV)	Detector	Neutron Source	Resolved (R) or Average (A) Resonance	Laboratory	Year	Reference	Results
F	20-110	NaI	VdG	R	Oak Ridge	1965	24	$\Gamma_{\gamma_1}(E1) \sim \Gamma_{\gamma_1}(M1)$
F,Na,Mg,Al,S,Cl	20-110	NaI	VdG	R	Oak Ridge	1967	26	
Mg,Si,P,S	20-80	NaI	VdG	R	Stockholm	1969	28	Transition to $5/2^-$ , $7/2^-$
Na	2.85	Ge(Li)	Chopper	R	Brookhaven	1969	28	
<sup>40,42,44</sup> Ca	10-60	NaI	VdG		Oak Ridge/ Lucas Heights		37	
Ca,Ti,Cr,Fe	5-100	Ge(Li)	VdG	R	Lucas Heights	1969	31	Transition to $5/2^-$ , $7/2^-$ p or d-wave capture
Mn	2.4	NaI	Chopper	R	Argonne	1958	60	$\Gamma_{\gamma_1}(E2) \sim X200 \Gamma_{\gamma_0}$ $\Gamma_{\gamma_1}(E1) \sim \Gamma_{\gamma_1}(M1)$
Mn	~ 2	Ge(Li)	Sc filter	R	Idaho Falls	1969	17	
Fe	1.17	Ge(Li)	Chopper	R	Brookhaven	1969	9	
Mn,Co,Cu	→ 10	Ge(Li)	Linac	R	Livermore	1968	29	Direct capture interference
Sc,V,Mn,Co	5-80	Ge(Li)	VdG	A	Lucas Heights	1969	31	Reduction in high energy intensity
Fe,Ni,Cu	10-60	NaI	VdG	A	Oak Ridge	1961	20	
Ni,Cu	15-300	NaI	VdG	A	Stockholm	1961/ 1962	19,61	Reduction in high energy intensity
<sup>54,56</sup> Fe, nat.	10-60	NaI	VdG	R	Oak Ridge/ Lucas Heights	1968	62	Transitions to $5/2^-$ , $7/2^-$
<sup>56</sup> Fe	0.7-70	( $\gamma_0, n$ )	Linac	R	Livermore	1967	63	$E_\gamma^3$ dependence
Cu	0.5-2.66	Ge(Li)	Linac	R	Harwell		30	
Cu	10-60	Ge(Li)	VdG	A	Lucas Heights	1968	21	
Ni	5-90	Ge(Li)	VdG	A	Lucas Heights	1969	47	Transitions to $5/2^-$
Zn	10-60	Ge(Li)	VdG	A	Lucas Heights	1969	31	Transitions to $\pm$ ve parity states
<sup>88</sup> Sr, <sup>90,91,92,94</sup> Zr	10-60	NaI	VdG	A	Oak Ridge		37	Transitions to $5/2^-$
Hf	2	Ge(Li)	Sc filter	A	Idaho Falls	1969	17	High energy enhancement independent of neutron energy
Ag,Sn,I,Cs	20-300	NaI	VdG	A	Stockholm	1962	48	
Ta	2	Ge(Li)	Sc filter	A	Idaho Falls	1969	17	5.5 MeV bump-independent of neutron energy
Ta,W,Au,Hg	15-300	NaI	VdG	A	Stockholm	1962/ 1964	49/ 50	
Pb,Ta,Au	15-4200							
Au	10-60	Ge(Li)	VdG	A	Lucas Heights	1968	56	Primary E1 gamma rays in bump
<sup>206,207</sup> Pb	10-100	NaI	VdG		Oak Ridge	1967	65	Direct capture interference ( $n, \gamma_0$ )
<sup>207</sup> Pb	41	NaI	VdG	R	Oak Ridge/ Lucas Heights		43	
<sup>207</sup> Pb	20-1500	( $\gamma_0, n$ )	Linac	R	Livermore	1969	44	
<sup>208</sup> Pb	41	( $\gamma_0, n$ )	Linac	R	Livermore	1969	45	Intermediate structure
Bi	1-12	( $\gamma_0, n$ )	Linac	R	Livermore	1968	63	Agreement with statistical model
<sup>238</sup> Hf	10-300	NaI	VdG	A	Stockholm	1962	64	

TABLE 2

## MULTIPOLARITY OF GAMMA RAY TRANSITIONS

## FOR CAPTURE IN EVEN-EVEN TARGETS

Angular Momentum $l_n$	Resonance $\omega$ State $J_f^{\pi}$ c	Final State			
		$1/2^-$	$3/2^-$	$5/2^-$	$7/2^-$
0	$1/2^+$	E1	E1	M2	E3
1	$1/2^-$	M1	M1	E2	M3
1	$3/2^-$	M1	M1	M1	E2
2	$3/2^+$	E1	E1	E1	M2
2	$5/2^+$	M2	E1	E1	E1

TABLE 3

TRANSITIONS TO  $5/2^-$  FINAL STATES

Compound Nucleus	Neutron Energy (keV)	Intensity (%)	Final State (keV)	Reduced Widths <sup>†</sup>	
				k(E1) x 10 <sup>-3</sup>	k(M1) x 10 <sup>-3</sup>
<sup>43</sup> Ca	AV	3	373	0.6	5
<sup>45</sup> Ca	AV	4	174	0.5	4
<sup>53</sup> Cr	30	18	1,007*	3.6	34
<sup>55</sup> Fe	AV	9	933	0.5	4.6
		4	1,322*	0.2	2.4
<sup>57</sup> Fe	26	3.3	706	1.6	15
	36	7.7	706	2.8	27
	52	8.4	135	2.4	23
		5.4	706	2.0	19
	72	12.6	135	3.6	35
		3.3	706	1.2	12
<sup>59</sup> Ni	AV	4	341*	0.2	2.0
<sup>61</sup> Ni	AV	12	69	1.4	14
<sup>65</sup> Zn	AV	2	g.s.	0.9	9.4
<sup>67</sup> Zn	AV	$\frac{1}{2}$	g.s.	0.1	1

\* Final State  $l_n = 3$ ,  $J_f^{\pi} = 5/2^-$  or  $7/2^-$

†  $\langle k(E1) \rangle = 1.5$ ;  $\langle k(M1) \rangle = 14.0$



TABLE 4

TRANSITIONS TO  $7/2^-$  FINAL STATES

Compound Nucleus	Neutron Energy (keV)	Intensity (%)	Radiation Width (eV)	Final State (keV)	Reduced Widths	
					$k(E1) \times 10^{-3}$ (d-wave)	$k(E2) \times 10^{-6}$ (p-wave)
$^{41}\text{Ca}$	73	4.0	1.0*	g.s.	0.3	0.3
	85	2.9	1.0*	g.s.	0.3	0.2
	105	10.0	1.0*	g.s.	0.9	0.7
$^{45}\text{Ca}$	AV	2	1.0*	g.s.	.04	0.3
	AV	1	1.0*	g.s.	0.2	0.15
$^{49}\text{Ti}$	38	$\leq 76$	1.0*	g.s.	$< 13.7$	$< 12.7$
$^{55}\text{Fe}$	AV	$> 2$	0.3	1,413	$> 0.1$	$> 0.1$
$^{57}\text{Fe}$	1.15	7	0.6	706	-	0.3

\* Assumed



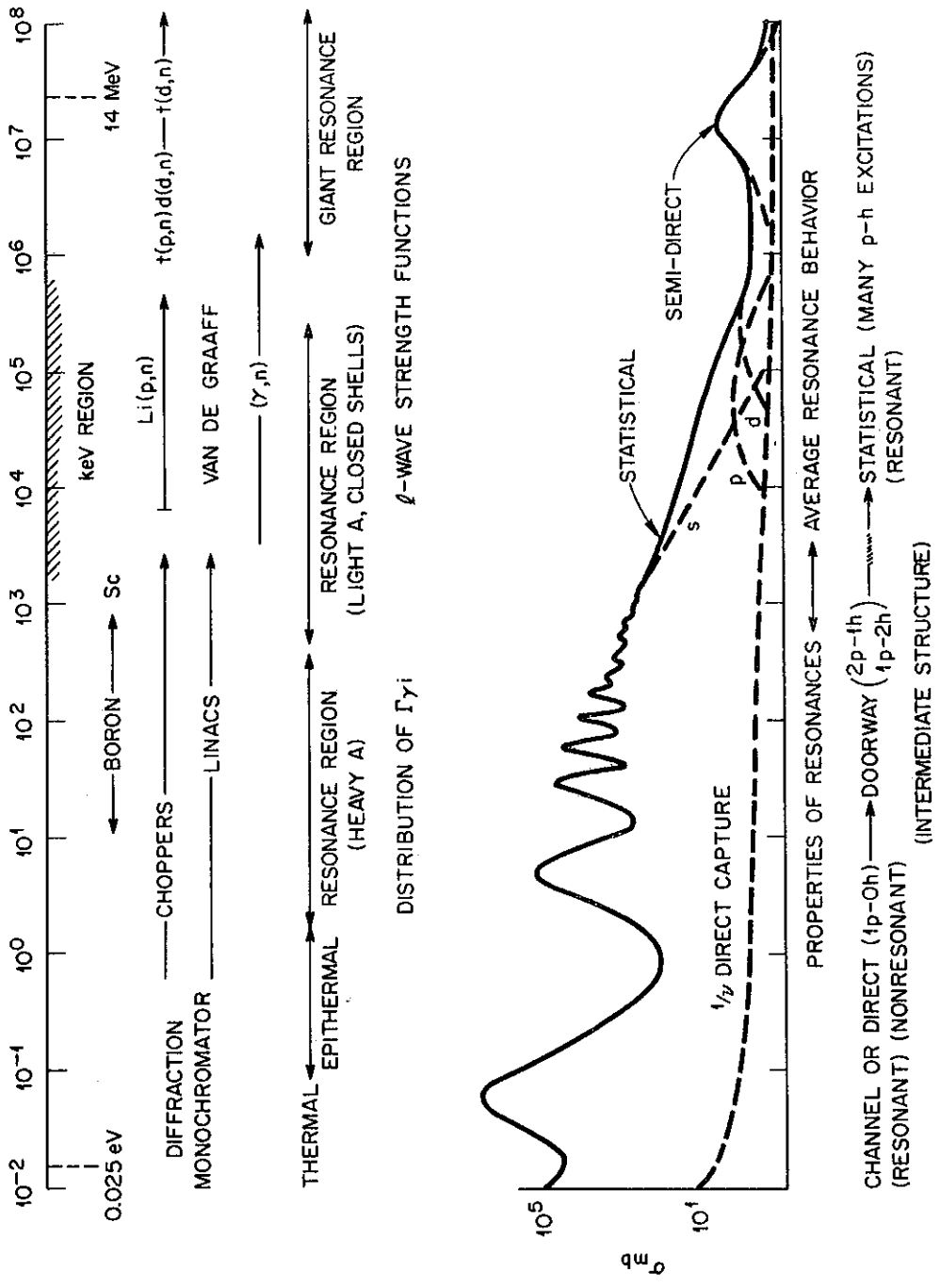


**FIGURE 1. NINE DECADES OF NEUTRON CAPTURE**

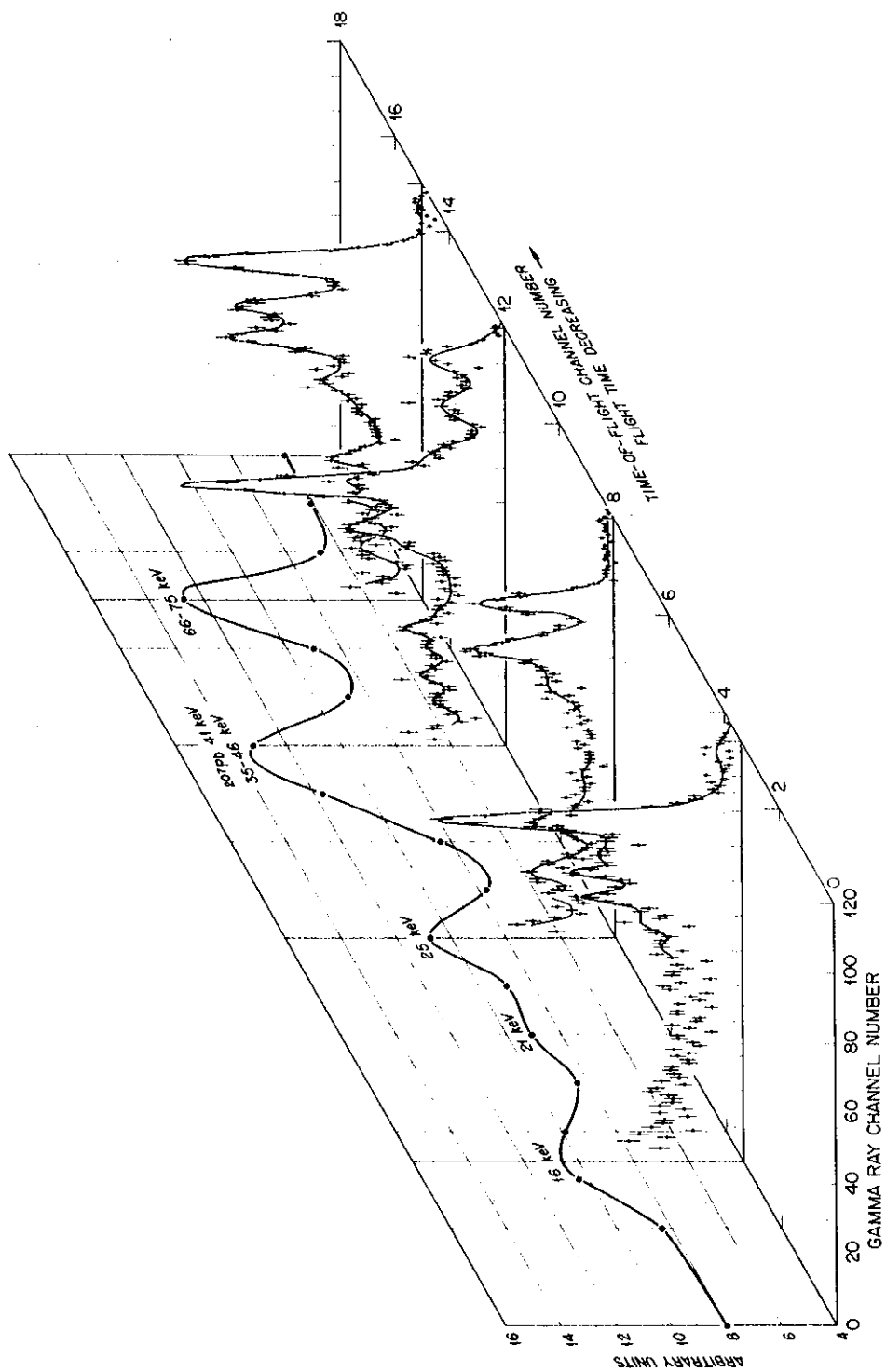


**FIGURE 2. RESONANCE CAPTURE GAMMA RAY SPECTRA IN  $^{206}\text{Pb}$**

Gamma ray spectra are obtained for each neutron resonance in this two parameter experiment.

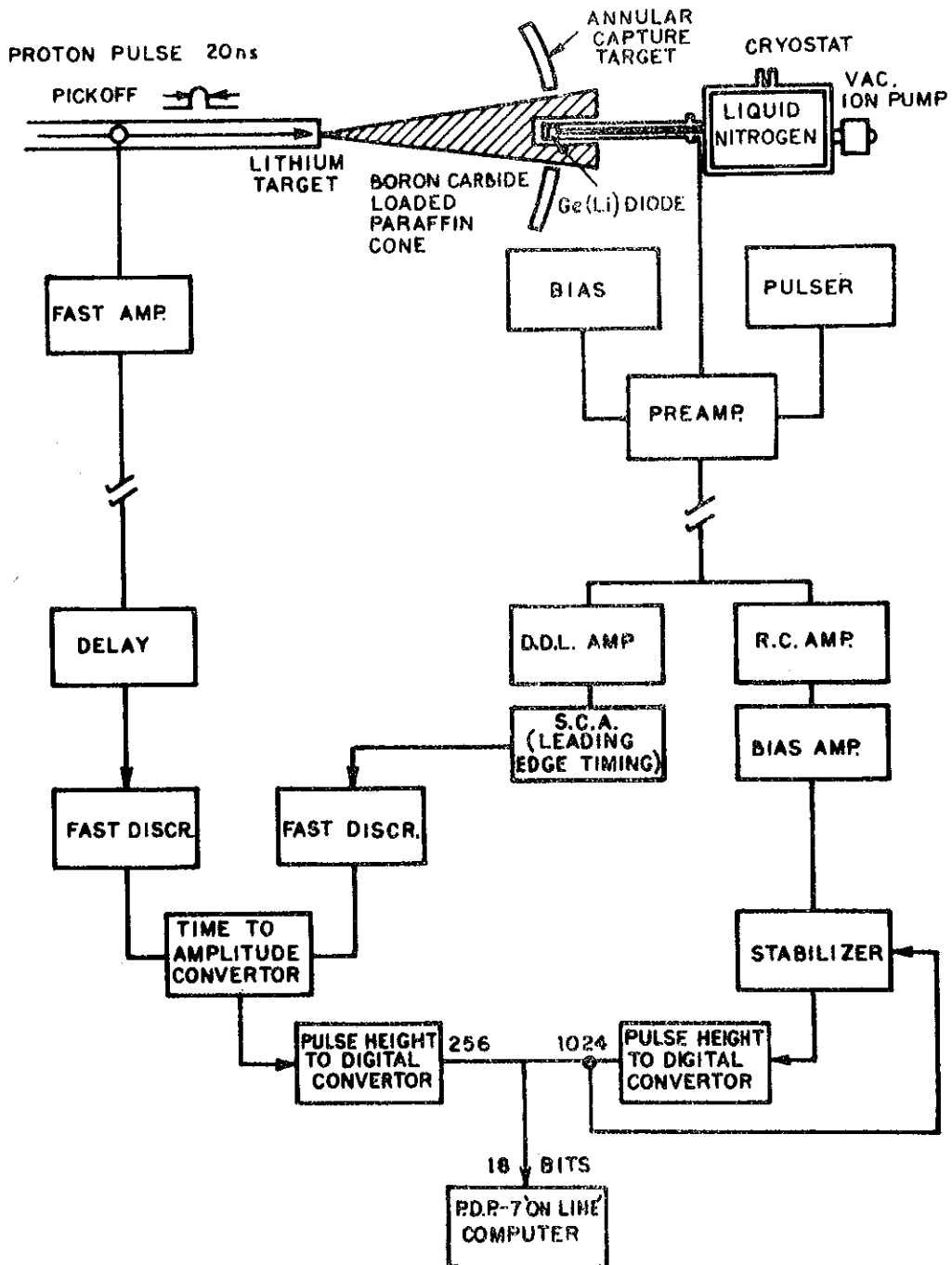


**FIGURE 3. DUAL PARAMETER SYSTEM FOR THE STUDY OF RADIATIVE keV NEUTRON CAPTURE**

Gamma ray and time of flight pulses are analysed in coincidence and processed by an on-line computer.

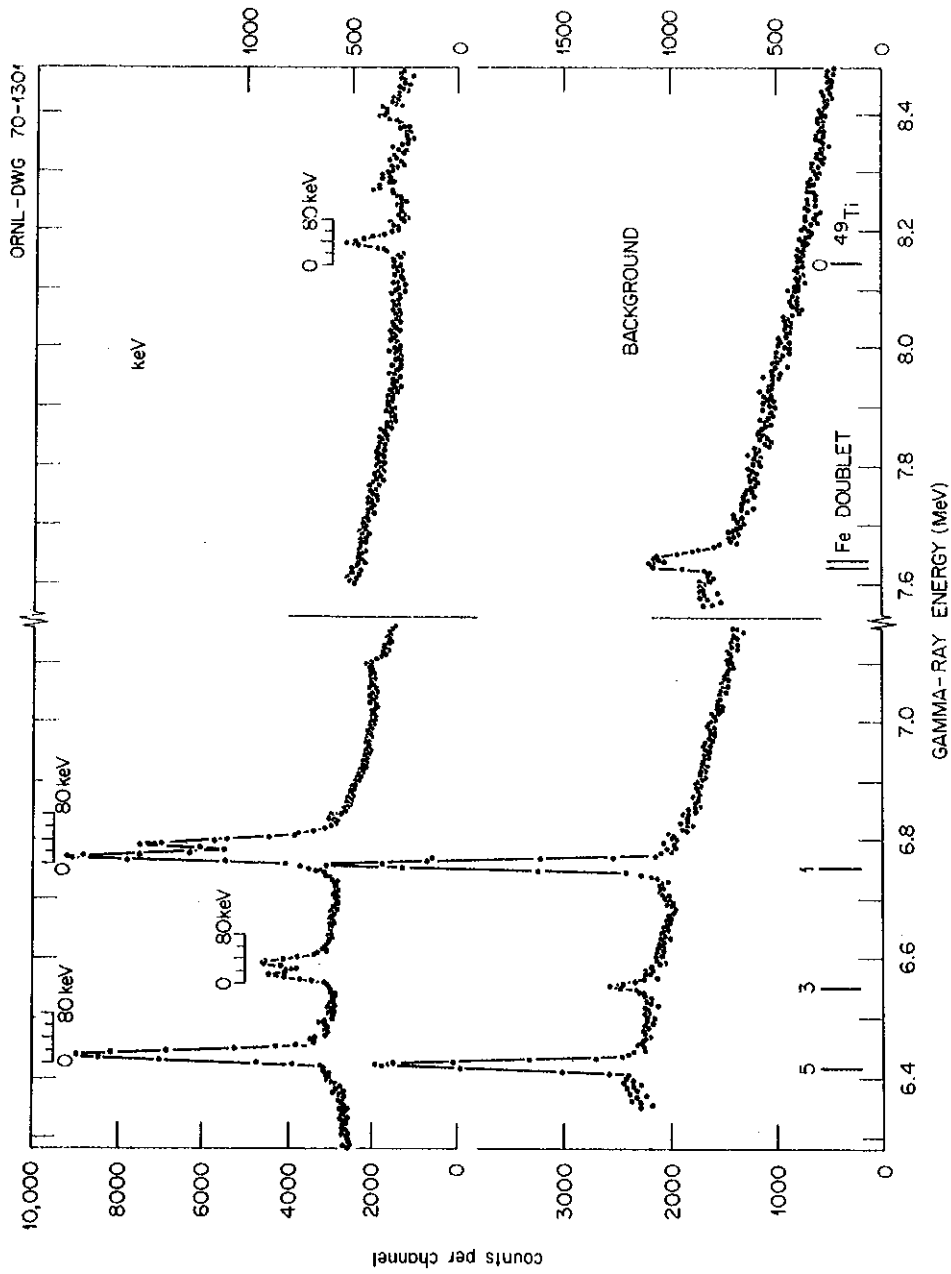


**FIGURE 4. THE  $^{48}\text{Ti}$  keV CAPTURE SPECTRUM**

The energies of the primary gamma rays from keV capture are shifted by the neutron resonance energies above the corresponding thermal (background) gamma ray energies.

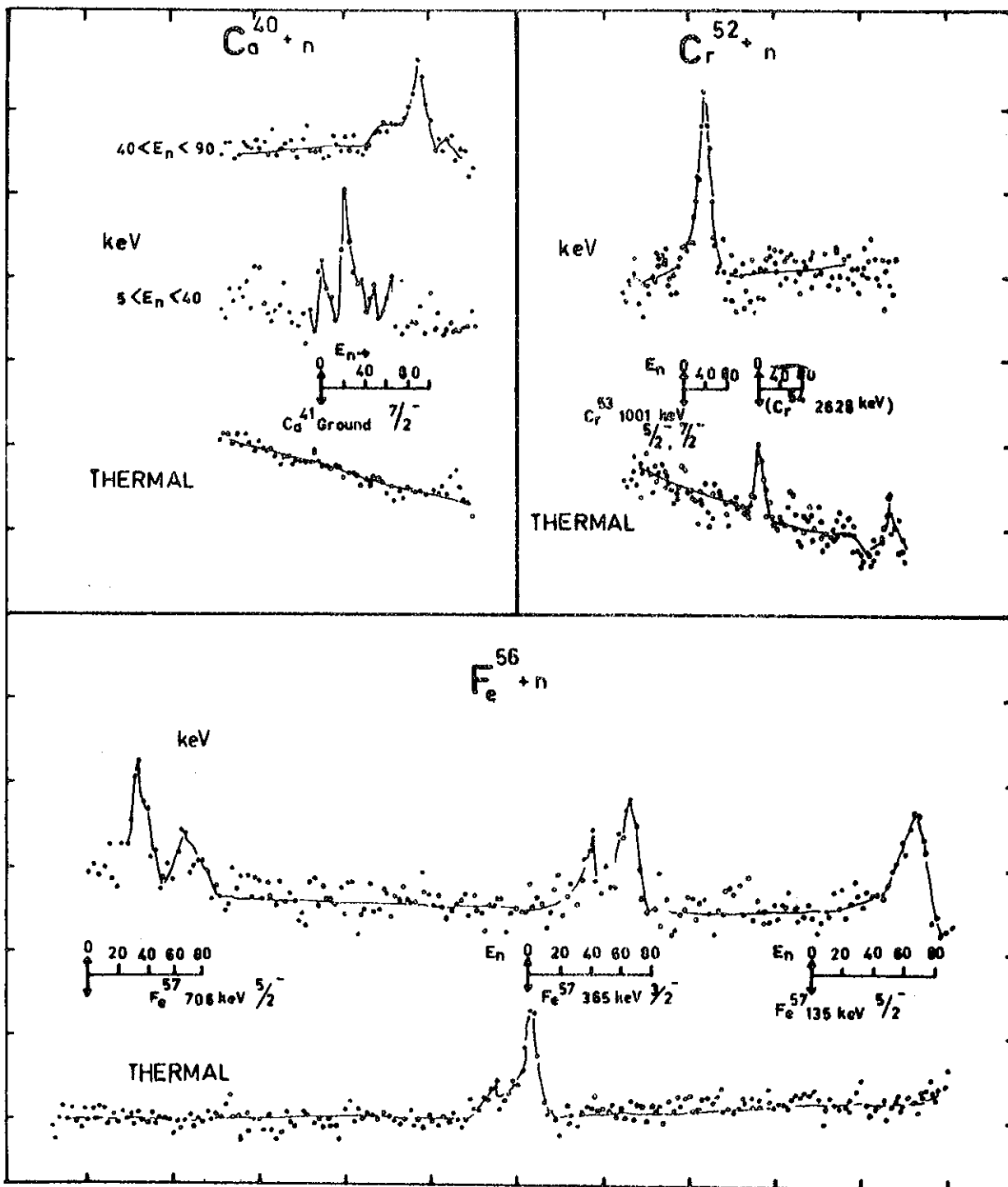
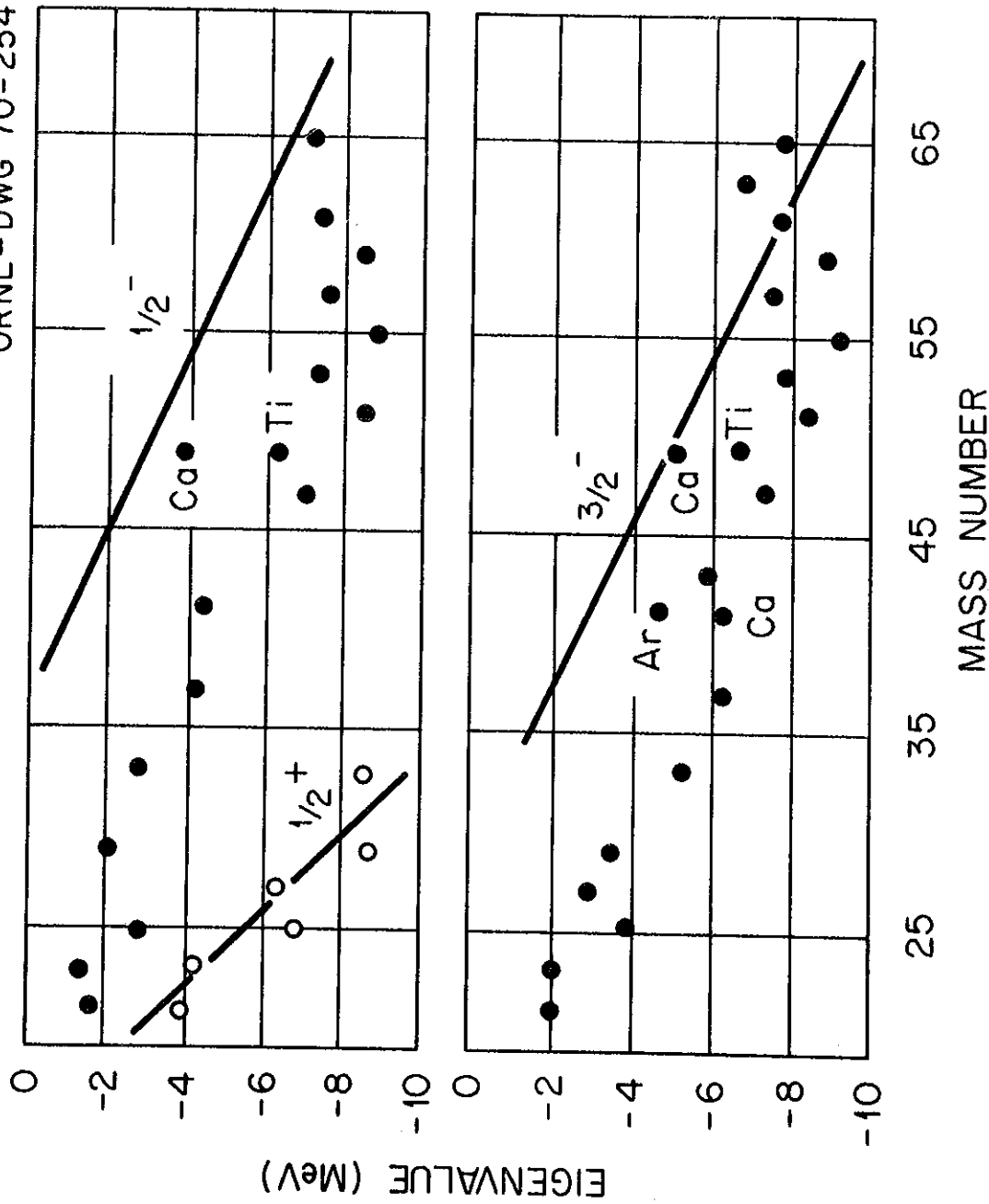


FIGURE 5. TRANSITIONS TO HIGH SPIN ( $5/2^-$ ,  $7/2^-$ ) FINAL STATES  
IN  $^{41}\text{Ca}$ ,  $^{53}\text{Cr}$ ,  $^{57}\text{Fe}$

These transitions are not seen in the corresponding portions of the thermal capture spectra.



**FIGURE 6. ENERGY EIGENVALUES FOR SINGLE NEUTRON STATES IN NUCLEI WITH  $20 < A < 65$**

Solid and open dots correspond to observed values for p and s final states which are populated most strongly in thermal and key capture respectively. Solid lines are calculated single neutron energies.



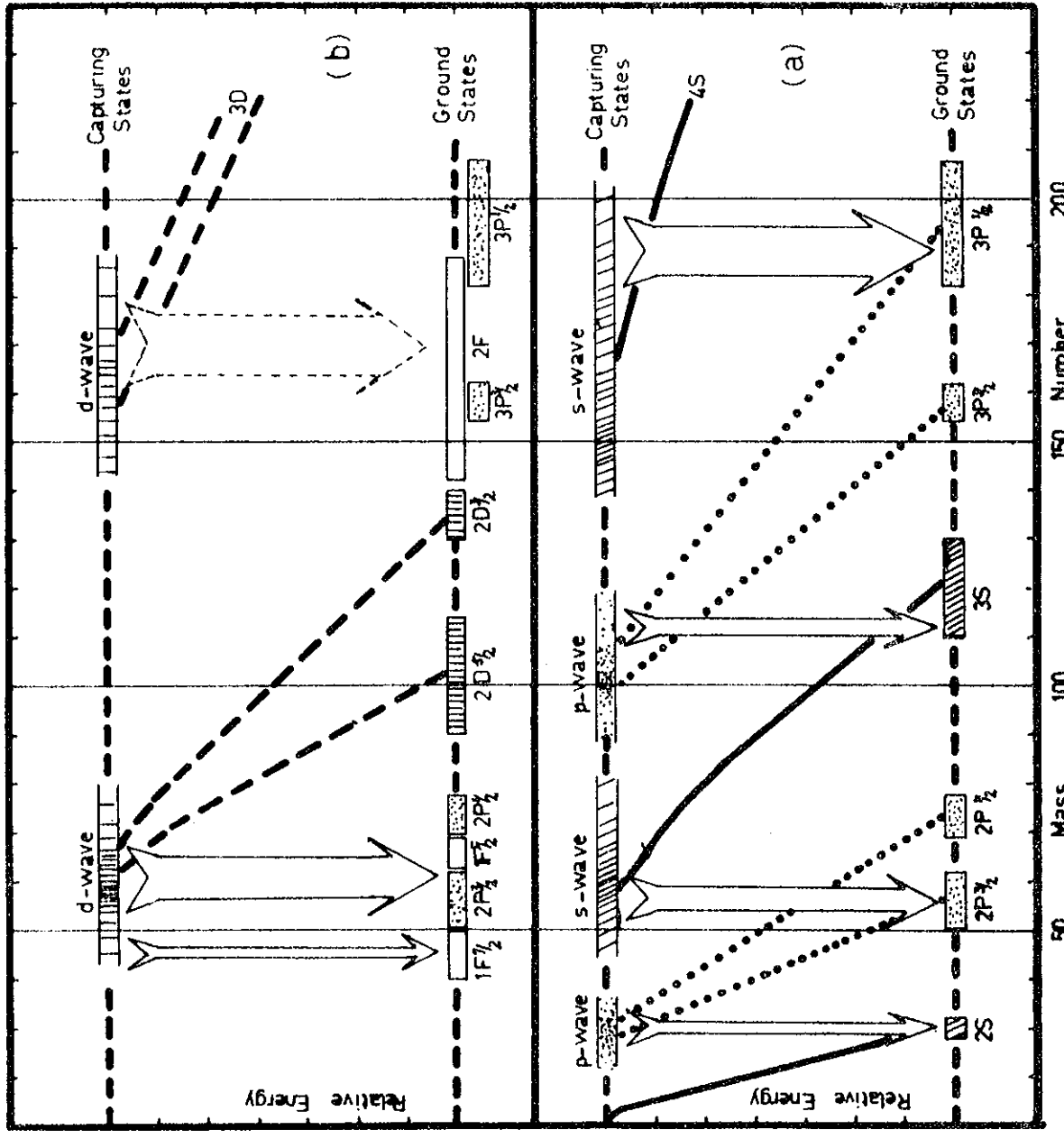
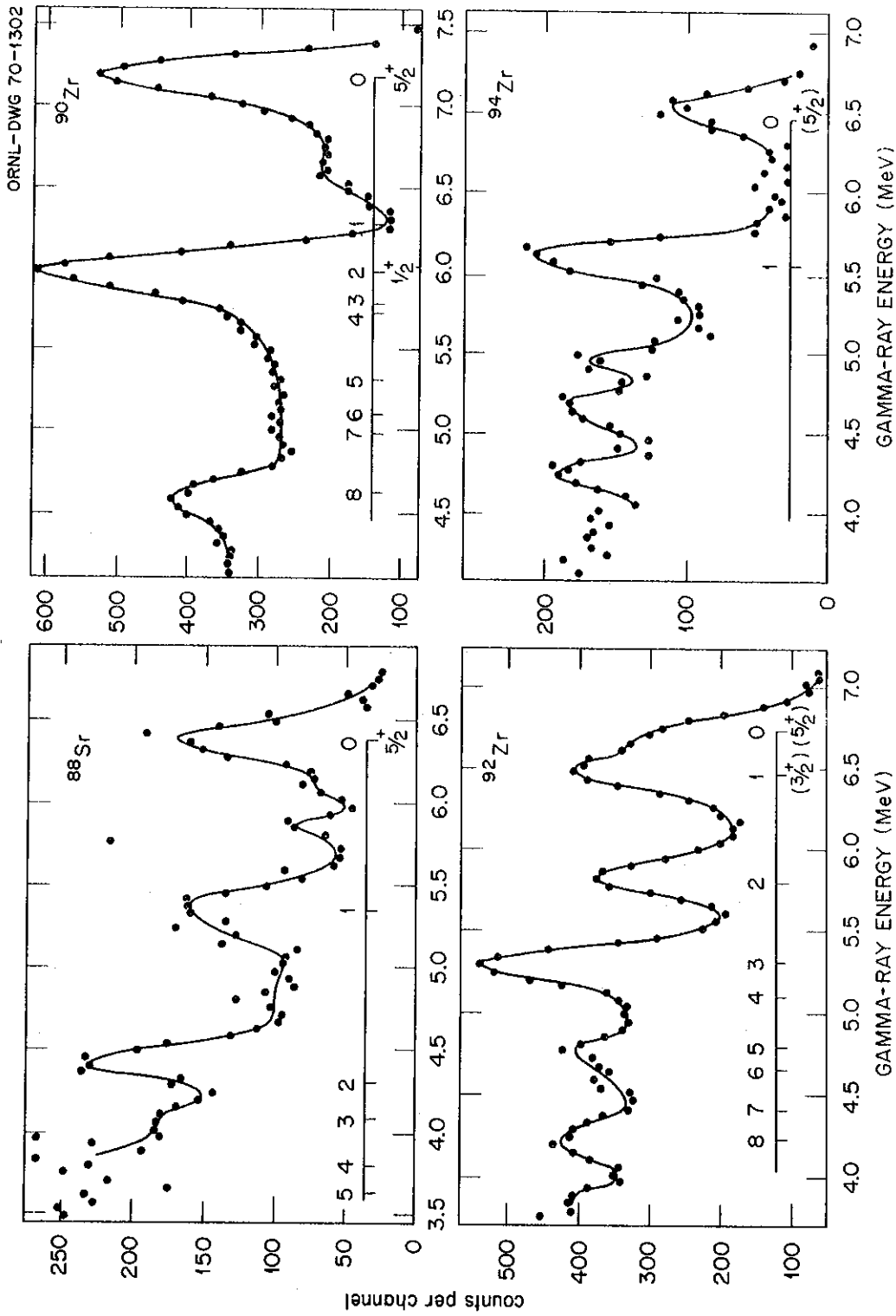


FIGURE 7. SCHEMATIC VARIATION OF NEUTRON STATES ACROSS THE PERIODIC TABLE

At the zero binding of neutron shells, the appropriate strength function maximises, and E1 transitions link low lying shells.



**FIGURE 8. THE keV CAPTURE SPECTRA FOR TARGETS OF  $^{88}\text{Sr}$ ,  $^{90}\text{Zr}$ ,  $^{92}\text{Zr}$ ,  $^{94}\text{Zr}$**

Strong transitions are observed to  $5/2^-$  ground states which are not observed in thermal capture.

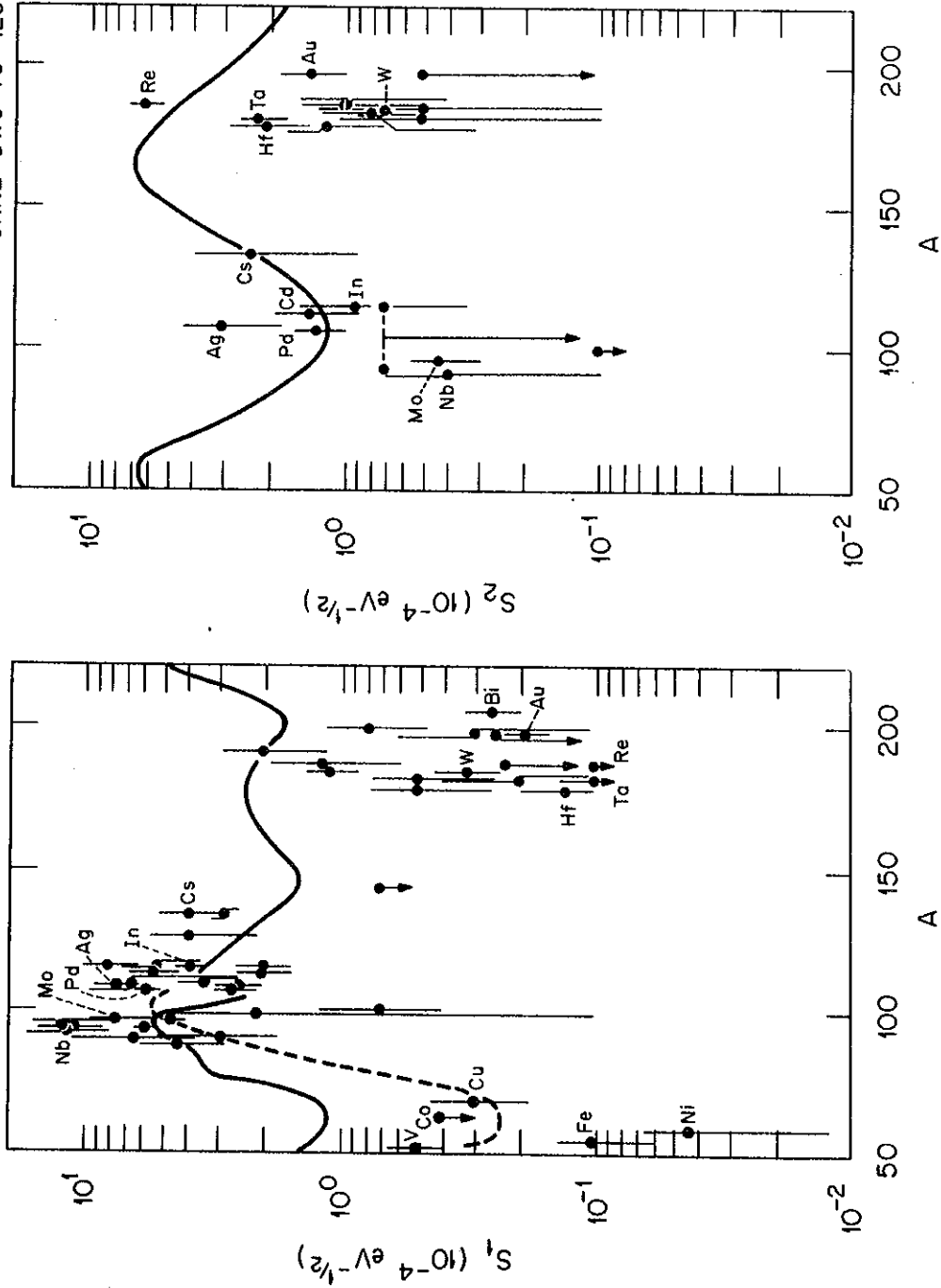


**FIGURE 9. THE P AND d-WAVE STRENGTH FUNCTIONS**

Optical model calculations deviate substantially from the scattered experimental data.

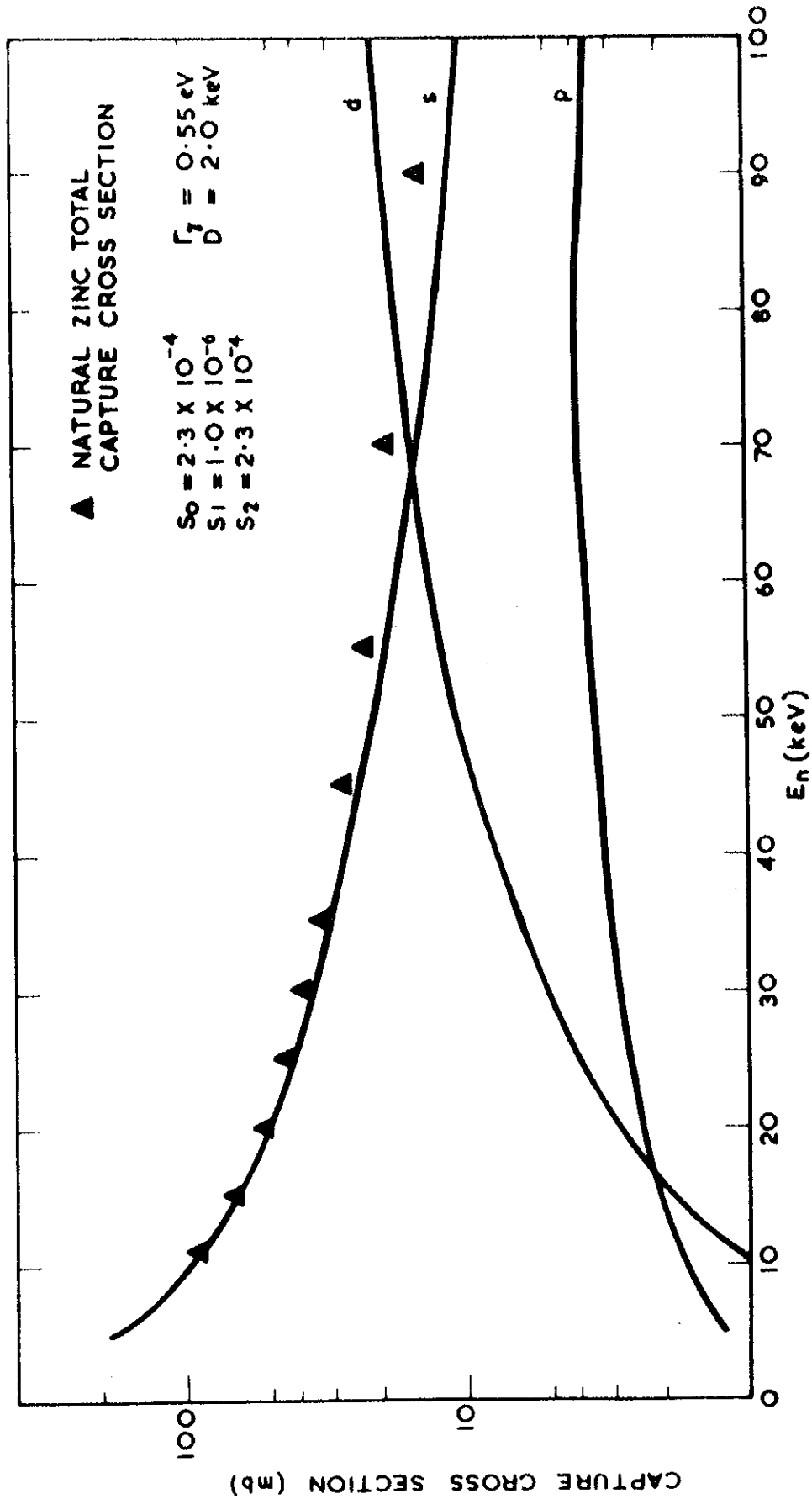


FIGURE 10. AN  $\ell$ -WAVE ANALYSIS OF keV CAPTURE CROSS SECTIONS IN Zn

To fit the energy dependence,  $S_2$  is required to be  $\sim$  zero. The derived value of  $S_2 \sim 2 \times 10^{-4} \text{ eV}$  results in the d-wave cross section exceeding the capture cross section above 70 keV.

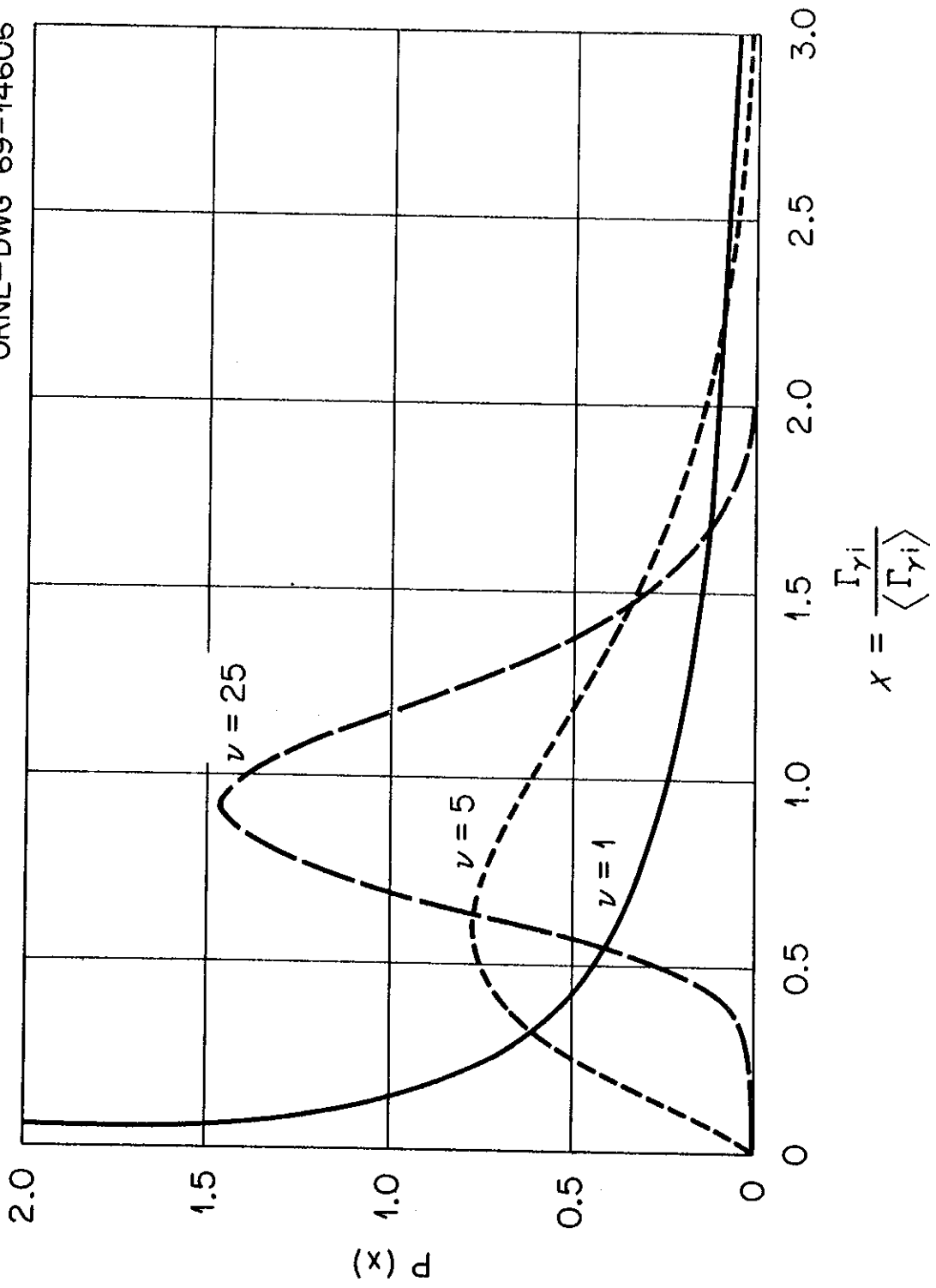
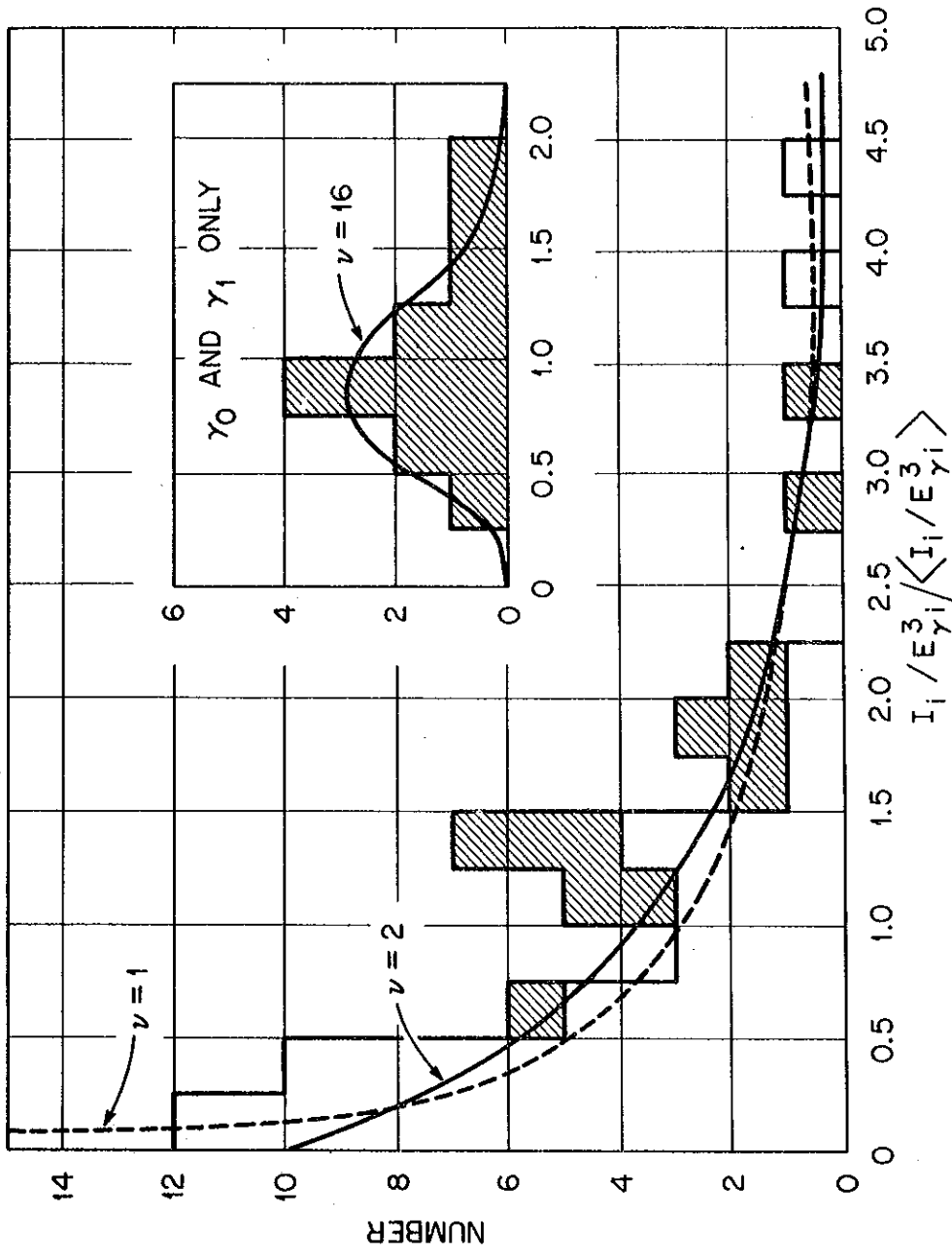


FIGURE 11. CHI-SQUARED DISTRIBUTIONS WITH 1, 5, AND 25 DEGREES OF FREEDOM



Distribution of Reduced Widths in  $^{57}\text{Fe}$ .

**FIGURE 12. DISTRIBUTION OF REDUCED PARTIAL RADIATIVE WIDTHS IN  $^{56}\text{Fe}$  ( $n, \alpha$ )**

Transitions to the ground and first excited state doublet exhibit strong correlations over a 75 keV energy range.

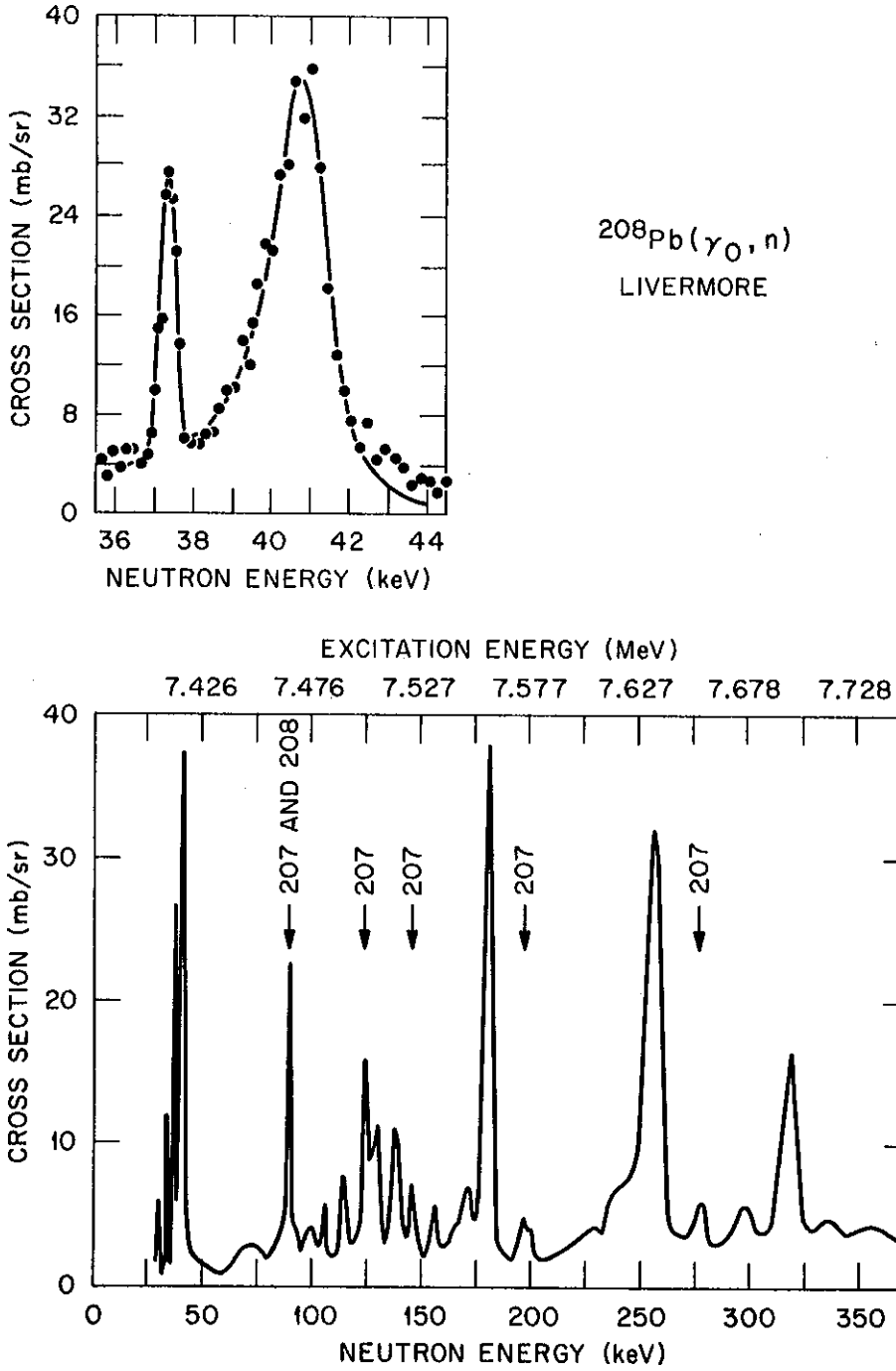


**FIGURE 13. PARTIAL CAPTURE CROSS SECTION FOR  $^{208}\text{Pb}(\gamma_0, n)$**

The asymmetry of the 41 keV resonance is interpreted in terms of a semi-direct interaction.

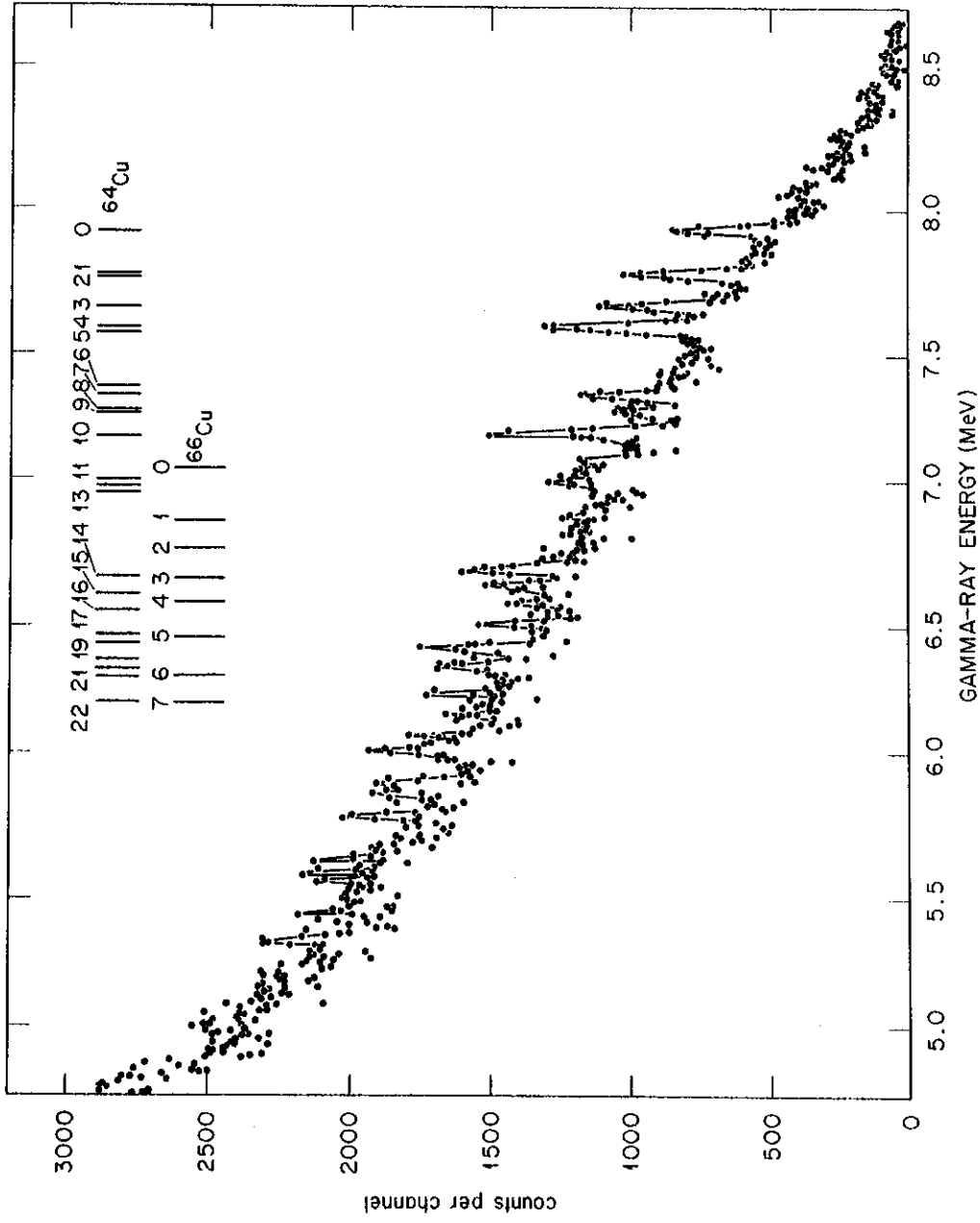


**FIGURE 14. THE 50 keV AVERAGED CAPTURE SPECTRUM IN Cu**

The uncertainty in the mean intensities is ~ 20%, and comparable to the experimental error. The high energy enhancement observed in thermal capture is not present in the keV region.



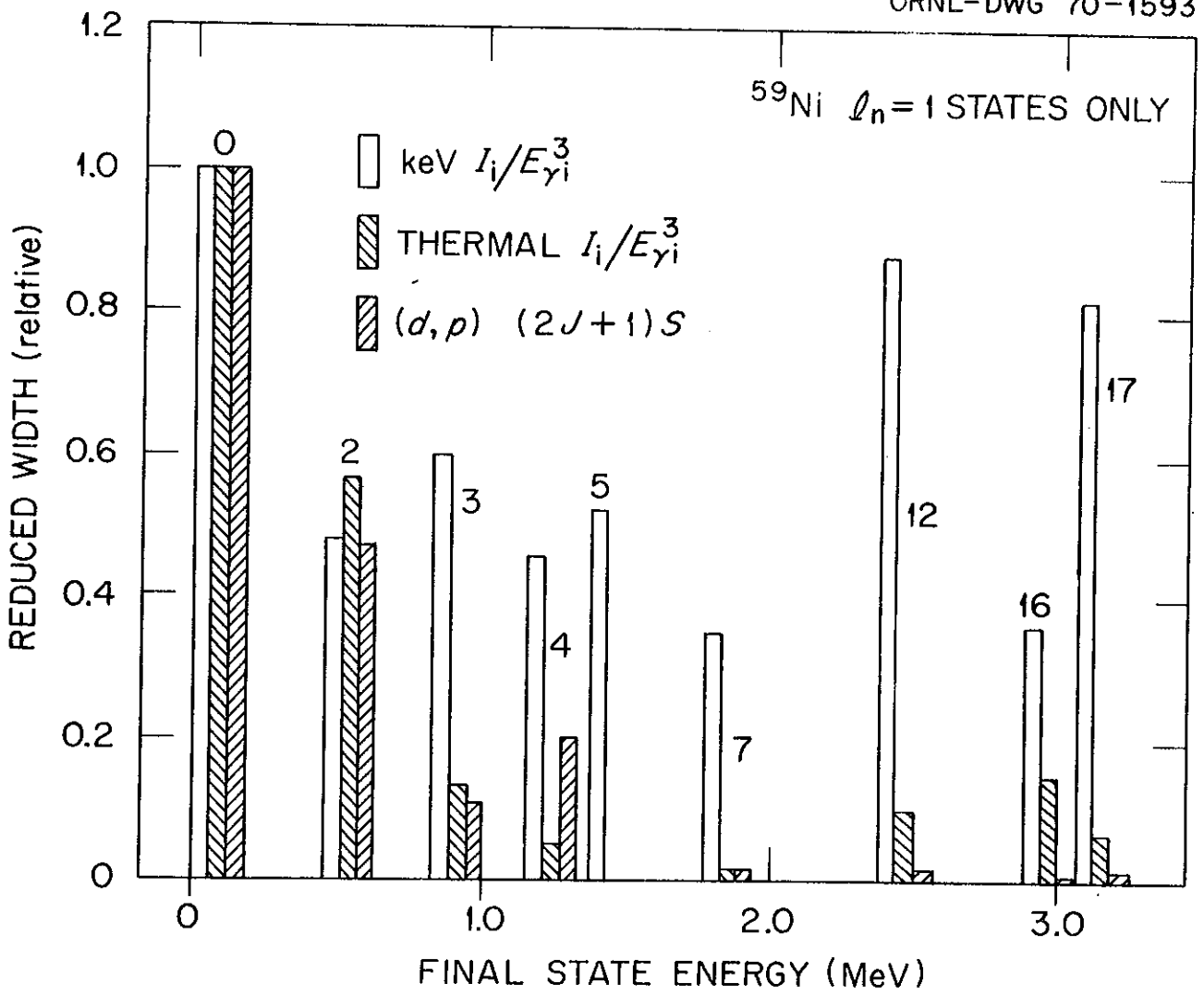


**FIGURE 15. COMPARISON OF REDUCED WIDTHS IN  $^{59}\text{Ni}$**

The correlation between (d,p) neutron widths and thermal capture radiative widths does not extend into the keV region.

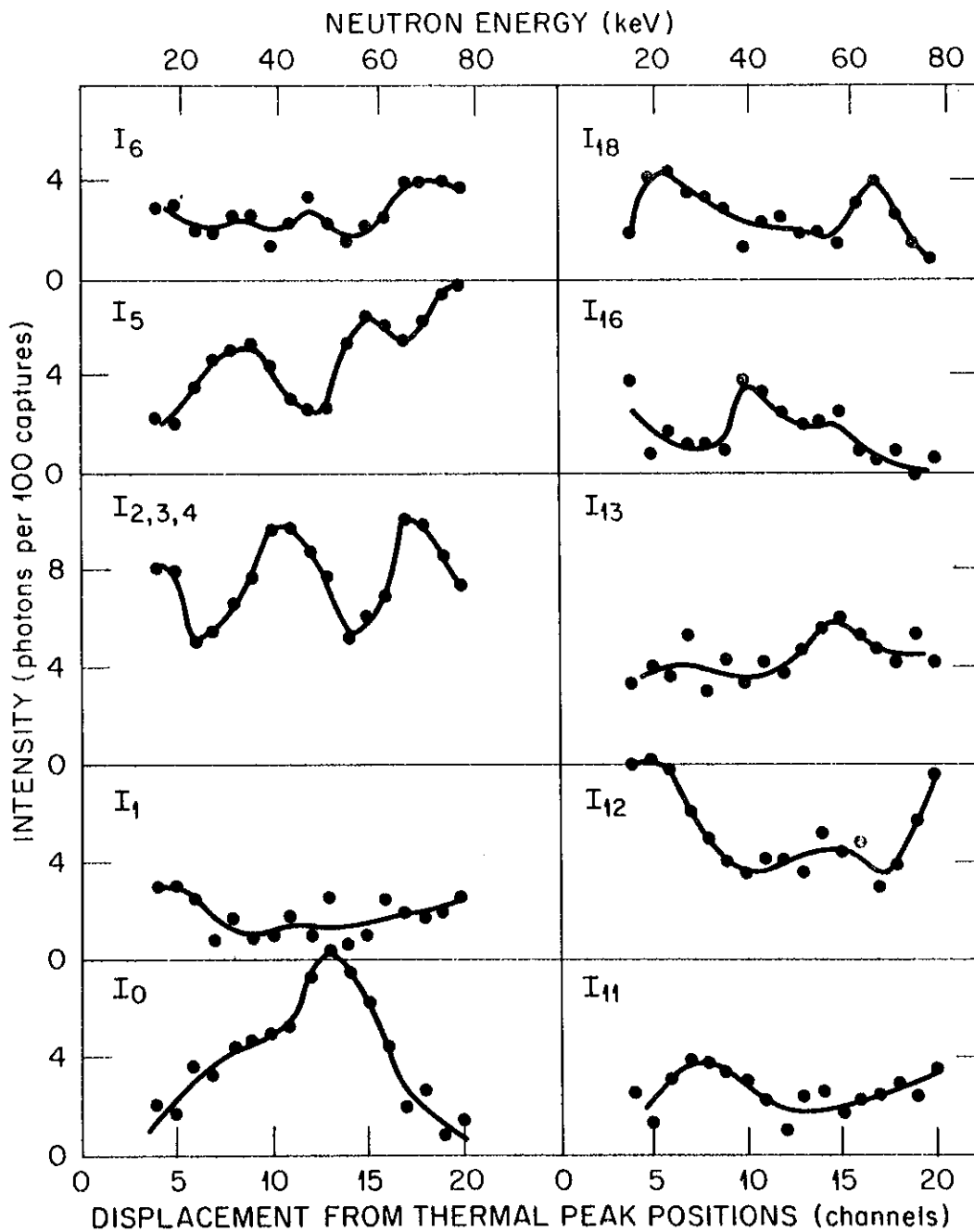


**FIGURE 16. VARIATION OF GAMMA RAY INTENSITIES WITH NEUTRON ENERGIES IN Co**

Intermediate structure with width 10 – 20 keV is observed, though the resonance spacing is only 1.4 keV.

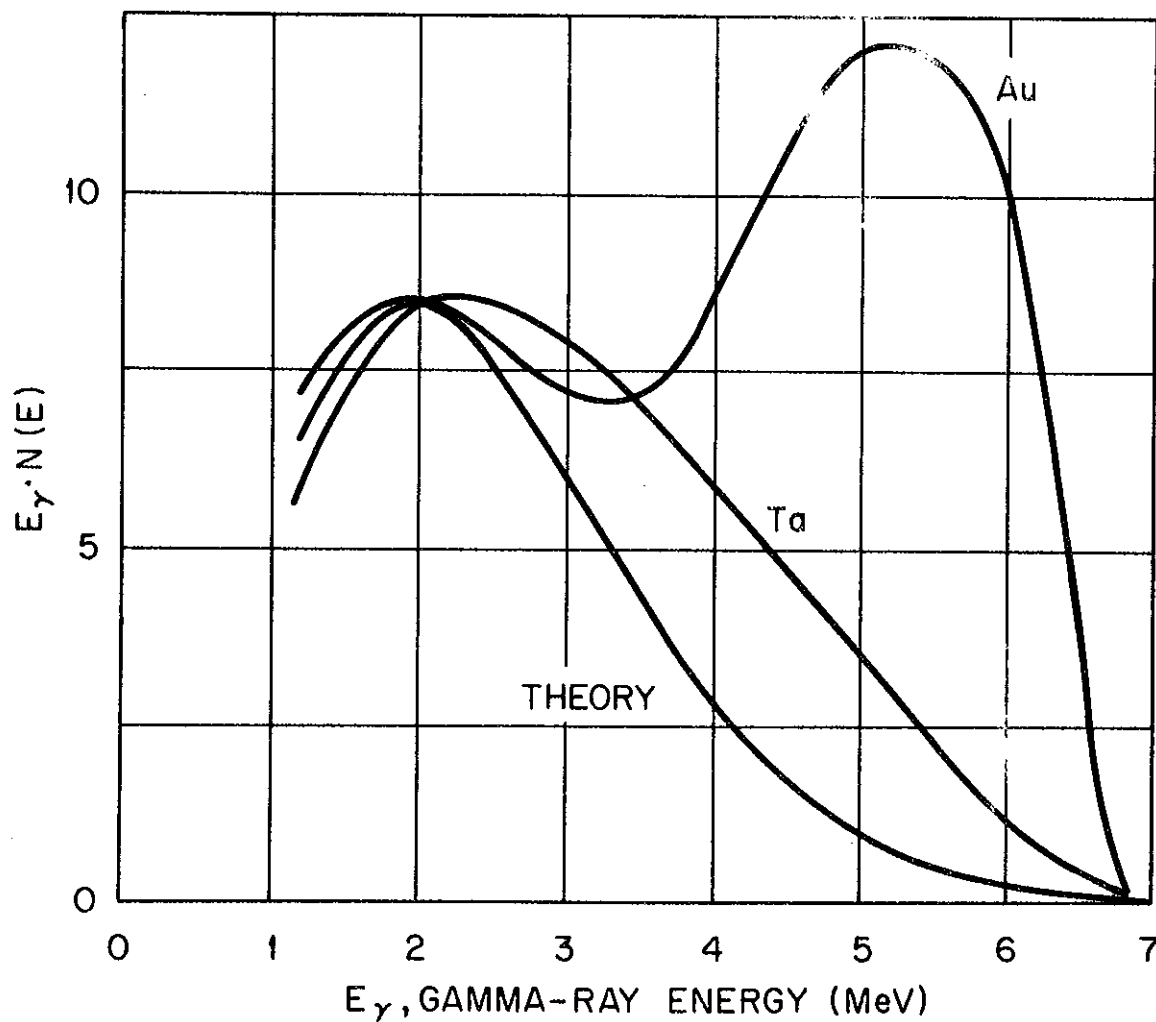


**FIGURE 17. AVERAGE NaI SPECTRA FOR  $k_eV$  CAPTURE IN Ta AND Au**  
 The calculated shape for a statistical model interaction is shown, and contrasts with the anomalous bump at 5.5 MeV.

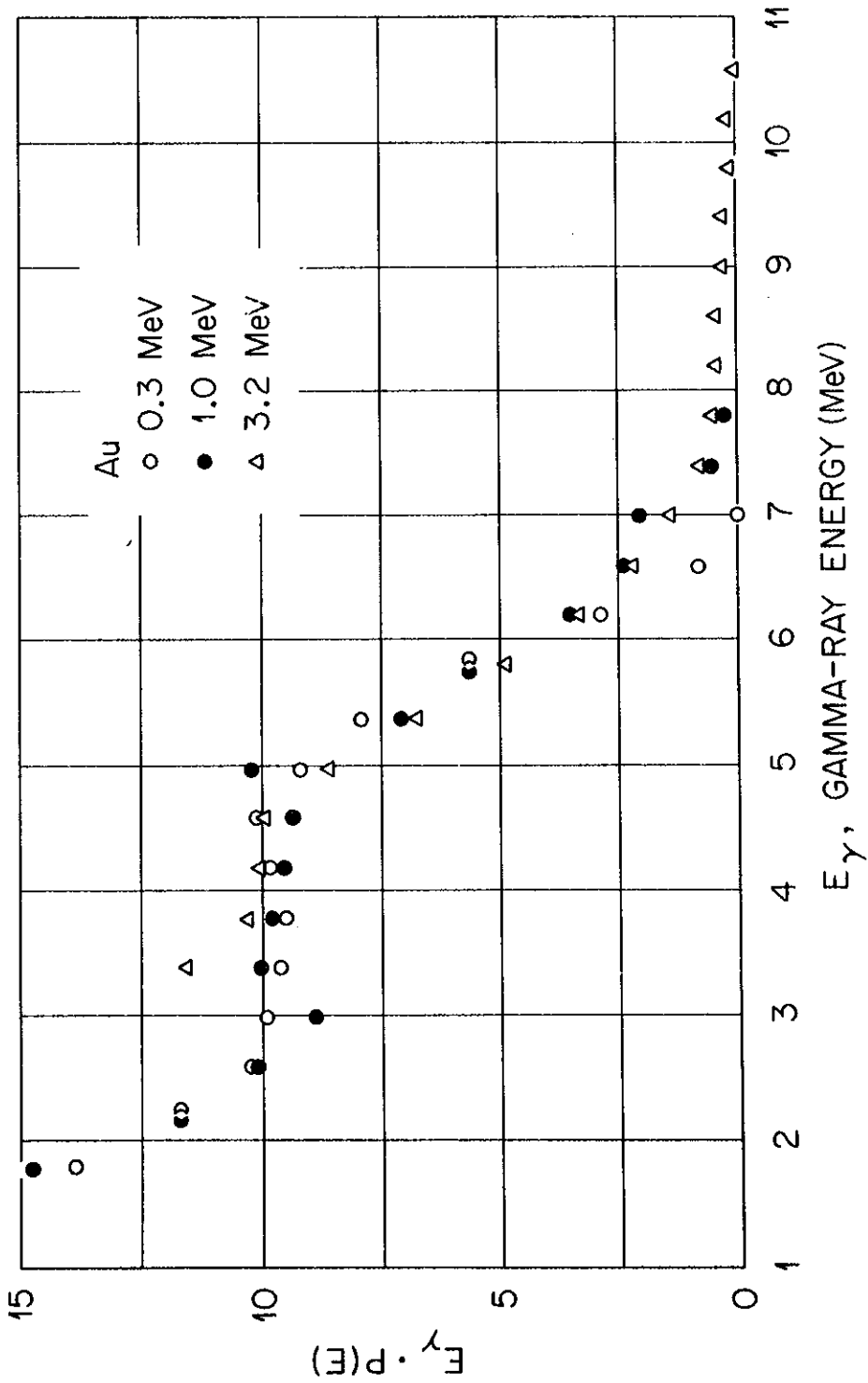


**FIGURE 18. AVERAGE CAPTURE SPECTRA IN Au**

The spectral shape is constant for neutron energies to 3.2 MeV.